Assessing separation processes for an aromatic and a chiral amine using Polybenzimidazole (PBI) membranes

Sara Alexandra da Silva Lopes

Thesis to obtain the Master Degree in

Bioengineering and Nanosystems

Supervisor(s):

Prof. Frederico Castelo Alves Ferreira
Dr.ª. Teresa Sofia Araújo Esteves

Examination Committee:

Chairperson: Gabriel António Amaro Monteiro
Supervisor: Frederico Castelo Alves Ferreira
Members of the Committee: Raquel Alexandra Morais Teixeira

December 2017

Acknowledgements

Quero agradecer aos meus orientadores, Professor Frederico Ferreira e Drª Teresa Esteves pela disponibilidade, orientação e apoio no desenvolvimento desta tese.

À Raquel por todo o apoio, ajuda e acompanhamento durante todo este processo. Ao professor Carlos Afonso por toda a ajuda, simpatia e acompanhamento durante a minha estadia na Faculdade de Farmácia.

Ao Flávio, porque sem ele o produto final não seria o mesmo. Obrigada pelo apoio constante, pela paciência, por estares disponível 24h por dia e por não me deixares baixar os braços. Queria também agradecer a contribuição com alguns dados experimentais incluídos neste trabalho e disponibilidade na execução de algumas tarefas.

Ana Teresa, obrigada por tudo, por seres a minha companhia todos os dias no laboratório onde construímos uma bela amizade, obrigada pela teu apoio incondicional e por me aturares dia e noite, foste um grande pilar.

Obrigada ao apoio incondicional dos meus pais e do meu irmão Valentim e por sempre acreditarem em mim.

E por fim, obrigada aos meus amigos, Amandine, Miguel, Joana, … por estarem sempre por perto e disponíveis para me apoiarem e dar-me força para nunca desistir dos meus objetivos.

Gostaria de agradecer financiamento de Fundação para a Ciência e Tecnologia (FCT) através de projecto SelectHost: Innovative and efficient platforms for the removal of genotoxic impurities, PTDC/QEQ-PRS/4157/2014**,**scholarshop SFRH/BPD/116767/2016 e iBB-Institute for Bioengineering and Biosciences (FCT reference: UID/BIO/04565/2013 and POL2020 reference 007317)**.**

Resumo

As aminas são intermediários químicos importantes utilizados na síntese orgânica e para a produção de compostos de interesse farmacêutico. Neste contexto, é importante desenvolver processos e técnicas de separação para purificar esses tipos de compostos. Dois tipos de processos de separação são abordados nesta tese: resolução de aminas quirais e remoção de potenciais impurezas genotóxicas presentes em ingredientes farmacêuticos ativos. Foram utilizadas duas aminas como modelo para os estudos desta tese: a lupanina, que é uma amina quiral e 4-dimetilaminopiridina (DMAP) é considerada uma impureza potencialmente genotóxica.

Vários processos foram desenvolvidos para resolver os problemas acima descritos, tais como resolução enzimática, cromatografia, nanofiltração e polímeros de impressão molecular. Esta tese explora o uso de um material, polímero de polibenzimidazole (PBI), em várias técnicas de separação. Foi utilizado com sucesso como adsorvente devido à sua capacidade de adsorção de aminas, em grânulos ou membranas ou foi usado como material para membranas impressas molecularmente, usadas em experiências de nanofiltração e adsorção.

As tentativas de fazer membranas impressas molecularmente para maiores eficiências de separação e de usar membranas para melhorar a resolução diastereomérica por recristalização de membrana provaram ser sem sucesso.

Além disso, avaliou-se a otimização da resolução diastereomérica, o que resultou em enantiomericamente a D- (+) - Lupanina pura usando ácido L-tartárico como agente de resolução. No entanto, utilizando o DTTA como agente de resolução, apenas um máximo de 89,16% de L - (-) - Lupanina foi obtido.

Também preparamos membranas impressas molecularmente com Lupanina para separar seus enantiómeros; No entanto, estes não foram eficientes para este fim.

Palavras-chave: Aminas, impurezas genotóxicas, ingredientes farmacêuticos ativos, polímero de polibenzimidazole, membranas de impressão molecular, resolução diastereomérica, lupanina, recristalização de membrana.

Abstract

Amines are important chemical building block used in the organic synthesis and for production of compounds of pharmaceutical interest. In this context, it is important to develop separation processes and techniques to purify these types of compounds. Two types of separation processes are addressed in this thesis: resolution of chiral amines and removal of potential genotoxic impurities present in active pharmaceutical ingredients. Two amines were used as model for these studies in this thesis: Lupanine is a chiral amine and 4-dimethylaminopyridine (DMAP) is regarded as a potentially genotoxic impurity.

Several processes have been developed to solve the above-described problems, such as enzymatic resolution, chromatography, nanofiltration and molecularly imprinted polymers. This thesis explores the use of a material, polybenzimidazole polymer (PBI), in various separation techniques. It was used successfully as scavenger, due to its ability to adsorb amines, either in beads or membranes or was used as a material to molecularly imprinted membranes, used in nanofiltration and adsorption experiments.

The attempts to make molecularly imprinted membranes for enhanced separation efficiencies and of using membranes to improved diastereomeric resolution by membrane recrystallization proved to be unsuccessfully.

Additionally, optimization of diastereomeric resolution was assessed, which resulted in enantiomerically the pure D- (+)- Lupanine using L-tartaric acid as resolving agent. However, using DTTA as resolving agent only a maximum of 89.16% of L-(-)- Lupanine was obtained

We also prepared membranes molecularly imprinted with Lupanine in order to separate their enantiomers; however these were not efficient for this purpose.

Key words: Amines, genotoxic impurity, active pharmaceutical ingredients, polybenzimidazole polymer, molecular imprinting membranes, diastereomeric resolution, Lupanine, membrane recrystallization.

Table of Contents

Acknowledgements ii

Resumo iii

Abstract iv

Table of Contents v

List of Figures vii

List of Tables ix

List of Abbreviations x

1- Aim of studies: Motivation and objectives 1

1- Introduction 2

1.1- Amines 4

1.1.1- Selected amines 5

1.1.1.1- Lupanine 5

1.1.1.2 -4-dimethylaminopyridine (DMAP) 7

1.2- Regulation in pharmaceutical industry 9

1.2.1- Regulation of chiral drugs 10

1.2.2- Regulation of genotoxic compounds 11

1.3- Separation methods 15

1.3.1- Chiral drugs 15

1.3.1.1- Diastereomeric resolution 16

1.3.1.2- Molecularly imprinted membranes (MIMs) 18

1.3.1.3- Membrane recrystallization 19

1.3.2- “Degenotoxification” 21

1.3.2.1- Organic solvent nanofiltration (OSN) 22

1.3.3- Freundlich and Langmuir adsorption isotherms and kinetics 24

1.4- Polybenzimidazole (PBI) role 27

2- Materials and Methods 29

2.1- Materials, equipments and analytical methods 29

2.2- Methods 30

2.2.1- Lupanine extraction 30

2.2.2- Polybenzimidazole treatment 30
2.2.3- Binding tests 32
2.2.3.1- Binding of Lupanine to PBI 32
2.2.3.2- DMAP and Meta mixtures 32
2.2.5- Molecularly imprinted membrane 33
2.2.5.1- Molecularly imprinted membrane manufacturing and pos treatment 33
2.2.5.2- Membrane adsorber 35
2.2.5.3- Nanofiltration 36
2.2.6- Diastereomeric resolution 37
3- Results and discussion 40
3.1- PBI as scavenger 40
3.1.1- Lupanine 40
3.1.1.1- Adsorption isotherms and kinetics 44
3.1.2- DMAP and Meta mixtures 46
3.1.2.1- Adsorption isotherms and kinetics 49
3.2- PBI membranes adsorbers 51
3.2.1- Lupanine 51
3.2.2- DMAP and Meta mixtures 52
3.2.3- PBI beads vs PBI membranes for DMAP and Meta 53
3.3- Nanofiltration with PBI membranes 54
3.4- Resolution by formation of diastereomeric salts with or without PBI membranes 59
3.4.1- Optimization of diastereomeric resolution by recrystallization using as resolving agent TA and DTTA without PBI membranes 59
3.4.2- Resolution by formation of diastereomeric salts with PBI membranes 64
Conclusion 65
References 66
Annex 71
Annex 1- Calibrations curves 71
Annex 2- Adsorption isotherms and kinetics 76
Annex 3- PBI modifications and possible chemical interactions with other molecules 82

List of Figures

Fig. 1 - Enantiomers of Thalidomide 3

Fig. 2-Chiral amine [8] 4

Fig. 3 - Quinolizidine ring structure 5

Fig. 4- (+)- Lupanine and (-)- Lupanine; Mw=248.36 g/mol 6

Fig. 5 – Meta (left) and DMAP (right) 8

Fig. 6 - DMAP-Catalyzed Sulfonylation during the Synthesis of Mometasone Furoate [2] 8

Fig. 7- Scheme of ICH process for the development guidelines based on [18] 11

Fig. 8- X-ray of the salt of (-)-lupanine and (+)-2,3-dibenzoyl-D-tartaric acid 17

Fig. 9- Scheme of molecular imprinting [35] 19

Fig. 10- Basic principle of separation by OSN. Solute rejection plotted against molecular size and weight. The small impurities pass through the OSN membrane, whilst the larger products are retained [38] 22

Fig. 11- Filtration cell [49] 23

Fig. 12- Polybenzimidazole (PBI) 27

Fig. 13 - Reaction scheme of the synthesis of PBI modified with 3-bromopropionic acid 31

Fig. 15- Process of phase inversion for membrane fabrication 33

Fig.16 - a) Adjust of casting knife above polypropylene non-woven support; b) Cast of membrane; c) Coagulation bath 34

Fig. 17- Dibromo-p-xylene (DBX) 34

Fig. 18- Scheme of cross-linked PBI with DBX 35

Fig.14- Membrane with HCl bath (right) and NaOH (left) 35

Fig. 19- Scheme of process of OSN 36

Fig. 20- L-tartaric acid; Mw= 150.09 g/mol 38

Fig. 21 -(+)- Lupanine and (-)- Lupanine; Mw=248.36 g/mol 38

Fig. 22- Di-p-toluoyl-L-tartaric acid and Di-p-toluoyl-D-tartaric acid; Mw= 386.35 g/mol 39

Fig. 23- Regeneration of PBI with DCM 43

Fig. 24 - Adsorption isotherm for binding of PBI-COOH with Lupanine in water 44

Fig. 25- Adsorption kinetics for binding of PBI-COOH with Lupanine in water 45

Fig. 26- Two forms of equilibrium for the protonated DMAP 47
Fig. 27- Regeneration of PBI with DCM 48
Fig. 28- Regeneration of PBI with MeOH 48
Fig. 29- Adsorption isotherm for binding of PBI-TA with DMAP in DCM 49
Fig. 30- Adsorption kinetics for binding of PBI-TA with DMAP in DCM 49
Fig. 31- Adsorption isotherm for binding of PBI-TA with Meta in DCM 50
Fig. 32- Lupanine adsorption with PBI membranes 51
Fig. 33 - Polystyrene 54
Fig. 34- Brilliant Blue 54
Fig. 35- Purpose of a chiral MIM 56
Fig. 37 - Rejection of the imprinted and control membranes measured in acetonitrile at 20 bar. 57
Fig. 36- Flux performance of the imprinted and control membranes measured in acetonitrile at 20 bar 57
Fig. 38 - Formation of salt complex between Lupanine and L-tartaric acid 60
Fig. 39 - Formation of salt complex between Lupanine and L-DTTA 62
Fig. 40- Illustration of recrystallization on membrane: membrane in contact with solution (left); formation of crystals (right) 64
Fig. 41 - Calibration curve of Brilliant Blue in MeCN 71
Fig. 42 - Calibration curve of Polystyrene 580 in MeCN 71
Fig. 43 - Calibration curve of Lupanine in H_2O for lower integrations of 24809353 u.a. 72
Fig. 44 - Calibration curve of Lupanine in H_20 for higher integrations of 24809353 u.a. 72
Fig. 45 - Calibration curve of DTTA 73
Fig. 46 - Calibration curve of Meta in DCM (concentration between 2.5 to 1000 ppm) 73
Fig. 47- Calibration curve of Meta in DCM (concentration between 1000 to 10000 ppm) 74
Fig. 48 - Calibration curve of DMAP in DCM (concentrations between 10 and 475 ppm) 74
Fig. 49- Calibration curve of L-tartaric acid in water 75
Fig. 50- Langmuir isotherm for binding of PBI-COOH with Lupanine in water 76
Fig. 51- Freundlich isotherm for binding of PBI-COOH with Lupanine in water 76
Fig. 52 - Pseudo first order kinetic for binding of PBI-COOH with Lupanine in water 77
Fig. 53- Pseudo second order kinetic for binding of PBI-COOH with Lupanine in water 78
Fig. 54- Langmuir isotherm for binding of PBI-TA with DMAP in DCM 78

Fig. 55- Freundlich isotherm for binding of PBI-TA with DMAP in DCM 79
Fig. 56- Langmuir isotherm for binding of PBI-TA with Meta in DCM 80
Fig. 57- Freundlich isotherm for binding of PBI-TA with Meta in DCM 81
Fig. 58- PBI-TB 82
Fig. 59- PBI-TA 82
Fig. 60- PBI-COOH 83
Fig. 61- PBI-COOH deprotonated 83
Fig. 62- PBI-COOH deprotonated with protonated Lupanine 84
Fig. 63- PBI-COOH deprotonated with Lupanine 84
Fig. 64- PBI-T with Lupanine 85
Fig. 65- PBI-T with Meta 85
Fig. 66- PBI-COOH deprotonated with DMAP protonated 86
Fig. 67- PBI-TB with DMAP protonated 86
Fig. 68- PBI-TA with DMAP 86

List of Tables

Table 1 - Classification of genotoxic impurities based on [22] 12
Table 2 - Allowable daily intake (µg/day) for genotoxic impurities during clinical development using the staged TTC approach [24] 13
Table 3- TTC staged limits proposed by the FDA [25] 14
Table 4 - Binding of Lupanine 41
Table 5- Possible chemical interactions between PBI-COOH and PBI-TA with lupanine (see annex 3) 42
Table 6 - Binding of DMAP and Meta 46
Table 7- Possible chemical interactions between PBI-TA, PBI-TB and PBI-COOH with DMAP 47
Table 8- Quantities of GTI and API adsorb by the membranes and percentage of adsorption 52
Table 9- Comparison between beads and membranes 53
Table 10- Comparison between beads and membranes for the same mass of PBI 53

Table 11 - Rejection value of Brilliant Blue and PS 580 in MeCN 55

Table 12- Sample of Lupanine with 1.1 mol equiv of L-tartaric acid 59

Table 13- Sample of Lupanine with D-DTTA and L-DTTA 61

Table 14- Samples of Lupanine with 1 mol equiv of L-DTTA in 2mL of acetone 63

Table 15- Samples of Lupanine with L-TA 64

Table 16- Parameters of the theoretical adsorption models obtained for a Lupanine solution in water with PBI-COOH 77

Table 17- Parameters of the theoretical kinetics models obtained for a Lupanine solution in water with PBI-COOH 78

Table 18- Parameters of the theoretical isothermic models obtained for DMAP in DCM with PBI-TA . 79

Table 19- Parameters of the theoretical kinetics models obtained for DMAP in DCM with PBI-TA 80

Table 20- Parameters of the theoretical isothermic models obtained for Meta in DCM with PBI-TA ... 81

List of Abbreviations

API	Active pharmaceutical ingredient
CHMP	Committee for Medicinal Products for Human Use
DBX	Dibromo-*p*-xylene
DCM	Dichloromethane

DIA	Drug Information Association
DMAc	Dimethylacetamide
DMAP	4-dimethylaminopyridine
DMSO	1,4 dimethylsulfoxide
DTTA	Di-p-toluoyl-tartaric acid
EC	European Communities
EWG	Expert working group
EMA	European Medicines Agency
e.e	Enantiomeric excess
FA	Formic acid
FDA	Food and Drug Administration
GTI	Genotoxic impurity
HBr	Hydrobromic acid
H_2SO_4	Sulfuric acid
H_2O	Water
HCl	Hydrochloric acid
HPLC	High-performance liquid chromatography

ICH	International Council for Harmonization
IPA	Isopropanol
KOH	Hydroxide Potassium
K_2CO_3	Potassium carbonate
MeCN	Acetonitrile
MeOH	Methanol
Meta	Mometasone Furoate
MIM	Molecularly imprinted membrane
MIP	Molecularly imprinted polymer
MTBE	Methyl tert-butyl ether
MWCO	Molecular weight cut off
NaOH	Hydroxide Sodium
Na_2HPO_4	Sodium Phosphate dibasic
Na_2SO_4	Sodium Sulfate
NF	Nanofiltration
NIM	Nom-imprinted membrane
N_2	Nitrogen

OSN	Organic solvent nanofiltration
PBI	Polybenzimidazole
PhRMA	Pharmaceutical Research and Manufacturers of America
ppm	Parts per million
PS	Polystyrene
TA	Tartaric acid
TTC	Threshold of Toxicological Concern

1- Aim of studies: Motivation and objectives

The aim of this study is to explore novel strategies to separate amines. Namely, to resolve Lupanine on its chiral enantiomers and to remove 4-dimethylaminopyridine (DMAP), a potential genotoxin, from an API post reaction stream. Considering processes of resolution of lupanine, different techniques, such as diastereomeric resolution by recrystallization, molecularly imprinted membranes and diastereomeric resolution assisted by membranes recrystallization were assessed.

Considering control of genotoxic impurity levels, removal of the genotoxic impurity was assessed by polymer adsorption methods using Polybenzimidazole (PBI) beads or membranes adsorbers.

To reach the objective of this thesis, several stages objectives were defined:

(i) pristine PBI beads, PBI conditioned with an alkaline or acid solution, and PBI with alkyl carboxylic groups were assessed for adsorption of lupanine in different solvents (water, acetonitrile and dichloromethane) and removal of DMAP from a mixture of DMAP/Mometasone Furoate (Meta) in dichloromethane.

(ii) PBI membranes adsorbers conditioned with alkaline or acid solution were used to study their adsorption capacity, for removal of DMAP or Meta from a DMAP/Meta dichloromethane solution.

(iii) molecularly imprinted membranes with lupanine, assess their rejection in organic solvent nanofiltration assays to evaluate their selectivity.

(iv) optimizing the lupanine diastereomeric resolution process by testing two chiral resolution agents, tartaric acid and Di-*p*-toluoyl-tartaric acid.

(v) membrane-assisted diastereomeric resolution of lupanine using PBI membranes and TA as resolving agent.

1- Introduction

Most pharmaceuticals are manufactured by applying an approach of total synthesis or modification of a natural product [1]. In both cases, a wide range of reactive molecules are used in synthetic reaction, many of these compounds are genotoxic or can form potential genotoxic compounds and thus may be present in the final active pharmaceutical ingredient (API) as impurities that can contaminate the final product and, ultimately reaching the patients. These type of impurities can induce genetic mutations, chromosomal breaks, and/or chromosomal rearrangements which can result in cancer in humans [2]. A wide range of unrelated chemicals, with very different structures and from very different chemical families, have been categorized as genotoxic impurities (GTI) [3]. The risk for the patient's health caused by the presence of impurities in APIs has become an increasing concern for pharmaceutical companies and regulatory authorities.

The development of simple and robust processes, using cost effective reagents to obtain high product yields through selective reaction and purification steps, is extremely important. The presence of GTIs can be avoided or mitigated by developing new synthetic route or Quality by Design (QbD) strategies which includes adjusting parameters such as pH, temperature, reaction time or matrix. Moreover, synthetic routes already include several APIs and API precursor purification steps, which offer several purge options for potential genotoxic impurities (PGTIS), still in spite of good practices in API synthesis development are enhanced purging of GTIS, there are cases in which addition separations steps may be necessary for GTI removal.

Other important separation in pharmaceuticals is resolution of chiral compounds. Optical isomerism was first observed by the French chemist Jean-Baptiste in 1815. However, Louis Pasteur is known as the founder of stereochemistry because, in 1948, he was able to separate for the first time the two isomers of sodium ammonium tartrate [4]. He found that optically inactive ammonium tartrate existed as a mixture of two types of crystals which were mirror images of each other so he proposed the existence of isomers that have differing mirror images with a difference in the direction of rotation of plane polarized light [4]. However, only about a century later, it was found that the phenomenon of chirality plays a key role not only in the life of plants and animals but also in pharmaceutical, agricultural and other chemical industries. In the pharmaceutical field, 56% of the drugs currently in use are chiral products and 88% of the last ones are marketed as racemic mixtures [5]. It is well established that the pharmacological activity is mostly restricted to one of the enantiomers (eutomer). In several cases, unwanted side effects or even toxic effects may occur with the inactive enantiomer (distomer). Even if the side effects are not that drastic, the inactive enantiomer has to be metabolized, representing an unnecessary burden for the organism [6].

When working with chiral molecules, which are identical but non-superimposable molecules, it is necessary to understand certain important concepts in this area. First of all, stereoisomerism, or chirality, refers to compounds with the same chemical formula but a geometrically different arrangement of the atoms in space, the so-called enantiomers. An enantiomer is one of two stereoisomers that are chiral, i.e., they are mirror images of each other. The nomenclature of the enantiomers uses (+) and (-) signs or d (dextro) and l (levo) or R and S. (+), d(dextro) or R means that the molecules rotate the plane of polarized light to the right (clockwise), whereas the and (-), l(levo) or S compounds make it rotate to the left or anticlockwise [4].

The issue of chirality has received special attention from the pharmaceutical industry after the thalidomide tragedy in the 1960s, when an unfortunate outcome of stereochemistry was revealed. Thalidomide was administered to pregnant women in the late 1950s in its racemic form to cure morning sickness. The consequence was birth defects and deaths as a result of the harmful S-isomer. The R-isomer was the effective drug. This tragedy has led to the approval of strict guidelines for the development of new drugs [4].

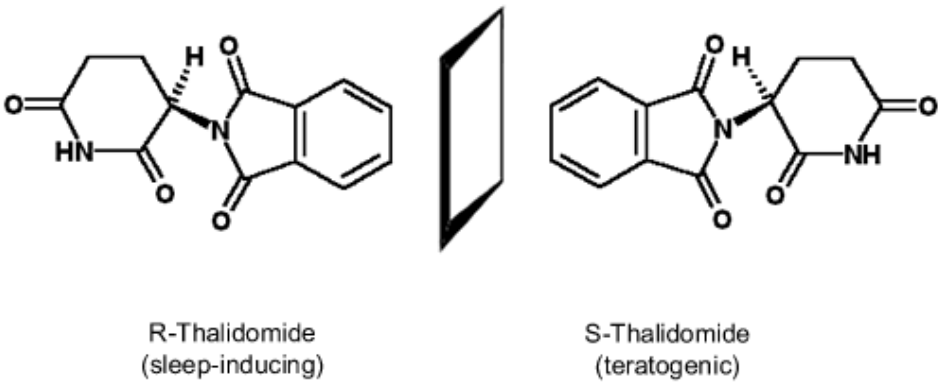

Fig. 1 - Enantiomers of Thalidomide

In the early 1980s, analytical chiral separation was a rather difficult task, and preparative synthetic and separation methods were not as advanced as today [7]. Nevertheless, it was clear that chiral drugs should be enantioseparated and that each enantiomer should be used separately. Nowadays, enantiomers are considered completely different compounds, as enantiomers of drug substances may have distinct biological interactions and, consequently, profoundly different pharmacological, pharmacokinetic, or toxicological activities.

1.1- Amines

Amines are a group of chemical compounds containing nitrogen atom that are sp3 hybridized with three single bonds to other elements. Although there are many different types of amines, they all have similar features because somewhere in their molecular structures they possess a nitrogen atom. The classification of primary, secondary, or tertiary refers to the number of organic groups that are attached to the nitrogen atom. If there is only one organic group, the amine is primary and has a general functional group of $-NH_2$. If there are two organic groups attached to the nitrogen atom, the amine is secondary and has a general functional group of –NH. If there are three organic groups attached to the nitrogen atom, the amine is tertiary and has a general functional group of simply –N.

The worldwide production of ammonia gas, and its use, can give an idea of the importance of amines, about 70% of it is used in the manufacture of fertilizers, 10% is used in the manufacture of nylon, 7% is used in the manufacture of explosives and the remaining 13% is used for the production of organic and inorganic chemicals.

Chiral amines have a stereogenic carbon at the α -position to the amino functionality (Figure 2).

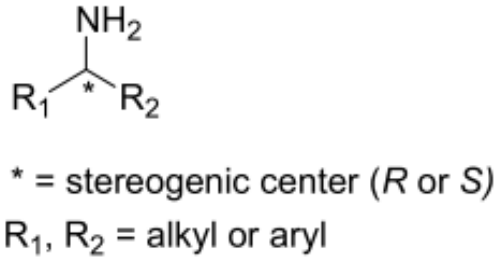

Fig. 2-Chiral amine [8]

Enantiomerically pure amines with an α-stereocenter play an important role in organic synthesis. They have a number of applications, such as chiral resolving agents, chiral auxiliaries, ligands in various asymmetric transformations, and advanced building blocks in pharmaceutical and agrochemical industries. They are also useful as chiral ligands in metal-complex catalysis [8]. Lupanine was the chiral amine chosen because it is a important building block for the synthesis of sparteine, an antiarrhythmic drug that is also employed in asymmetric synthesis [9].

1.1.1- Selected amines

1.1.1.1- Lupanine

The “lupin alkaloids” are found in a wide variety of plants and small trees, such as broom, lupin, gorse, and laburnum, which are used diversely in gardens, for fodder, and as sand-binders. The alkaloids are a group of molecules that are generally, toxic, but each individual molecule may be useful for veterinary pharmaceuticals and in insecticide manufactures. Chemical similarity rather than plant distribution issue to group these molecules under the category of alkaloids, since most of them contain-in actual or modified form-the quinolizidine ring structure (Fig.3).

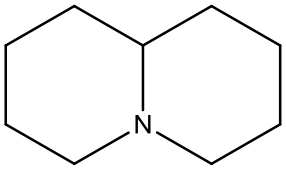

Fig. 3 - Quinolizidine ring structure

This basic quinolizidine ring was unknown prior to its discovery in the common lupin alkaloids : lupinine, cytisine, sparteine, lupanine, and anagyrine [10]. Because of their toxicity and bitter taste, alkaloids are a relevant limiting factor in the acceptation of *Lupinus* for consumption. Normally, these plants have 2% of alkaloids, mostly lupanine, sparteine, multiflorine, lupinine, anagyrine [11].

Lupanine (Fig.4) is a lupin alkaloid available in relatively high quantities in lupin beans (*Lupinus genus).* Lupin is actually a contaminant in the wastewaters from factories processing lupin seeds for human consumption. In fact, throughout history and around the world, plants containing alkaloids have been used to improve health and lupanine has some beneficial properties. For example, it can reduce blood glucose levels similarly to antidiabetics and some authors argue that lupanine can be used to correct arrhythmias. It can also be used to attack herbivores and as prevention against a wide range of insects. Lupanine is toxic to other animals, as well, since it is a very active neurotransmitter for nAChR (nicotinic acetylcholine receptor), which is crucial for neuronal signal transduction [12].

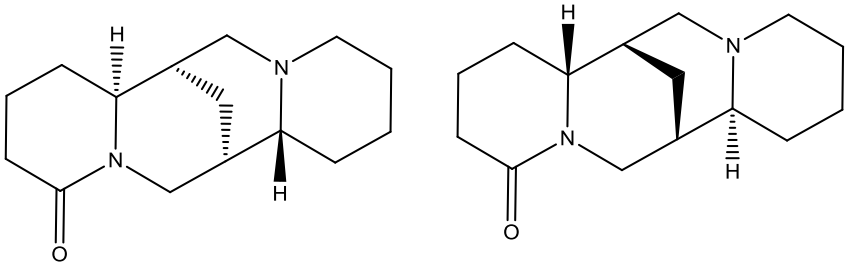

Fig. 4- (+)- Lupanine and (-)- Lupanine; Mw=248.36 g/mol

Lupanine and Sparteine, two prominent members of the tetracyclic quinolizidine alkaloid family, are important pharmaceutical compounds and enjoy considerable popularity in synthesis. L-(-)-Sparteine is widely employed as ligand or promoter for various asymmetric reactions due to its unique chiral diamine backbone.

The (+)-enantiomers of sparteine derivatives can be obtained by synthetic modification of (+)-lupanine by introducing selected substituents [13].

The resolution of Lupanine using a chiral acid as resolving agent in diastereomeric resolution by recrystallization is reported by Clemo et. al. (J. Chem. Soc. 1931, 429-437) who demonstrated the resolution of Lupanine with L-camphorsulphonic acid and D-camphorsulphonic acid to obtain L-(-)-Lupanine and D-(+)-Lupanine in 9.4% and 13% yields, respectively. More recently, Przybyl et al. (Tetrahedron 2011, 67,7787-7793) improved this resolution process significantly by using dibenzoyltartaric acid. Maulide and Afonso described an easier and more efficient process to extract, isolate and resolve *rac*-Lupanine into both enantiomers [14]. The inventors surprisingly found that a simple treatment of raw lupine seeds in alkaline solution at a pH of more than 12, followed by extraction and formation of diastereomers of lupanine, with L- tartaric acid, allow to obtain pure enantiomers of Lupanine. They also found that an increased yield of the desired enantiomer can be obtained by adding the dissolved Lupanine to a solution of the chiral acid, instead of adding the chiral acid to a solution of Lupanine. Using 0.75 molar equivalents of L-tartaric acid, in the resolution, they obtained the best result: a yield of 29% and an enantiomeric excess of 99.0% of D-(+)-Lupanine.

1.1.1.2 -4-dimethylaminopyridine (DMAP)

Genotoxins compounds have different structures and belong to different chemical families. From a chemical point of view, GTIs do not have physical-chemical properties or common structural elements that allow quick and easy identification. There are some molecules whose genotoxic effect is known, while others are classified as potential genotoxin due to the presence of reactive groups that can lead to genotoxicity; these reactive groups are cataloged as "structural alerts" [15].

Reactants used in chemical synthesis are usually selected due to their appropriate reactivity; however, this very same reactivity sometimes results in genotoxicity. Often such reactants are not fully consumed, persist in the reaction mixture, and can be carried forward in the reaction sequence. Genotoxins can also be present because they are used as catalysts, solvents or they may be present as API precursor by or side reaction molecules. Aromatic amines are a class of reactants commonly used in the production of API's. Although, generally they are not inherently genotoxic, they can become during metabolic activation, where electrophilic species are generated. The main transformation pathway of aromatic amine metabolism is oxidation, producing an N-hydroxy compound that is conjugated as an acetate, sulfate, or glucuronide.

Aminopyridine derivates are commonly used as started materials and catalysts in API synthesis. The derivative 4-dimethylaminopyridine (DMAP) is for example as the catalyst for synthesis of glucocorticoids, acylations, amino-group protection, esterifications, and sylilations but contains alerting genotoxic structures [16]. DMAP has a relatively high toxicity, corrosive and is particularly dangerous because of its ability to be absorbed through the skin [17]. DMAP can also enhance formylation, carbamoylation, benzoylation, tritylation, silylation, esterification, phosphorylation, polymerization of amides, esters, urethanes and many other reactions. DMAP (fig.5) finds uses in the synthesis of many pharmaceuticals, agrochemicals and general fine chemicals as well as in the flavor and fragrance, photographic, cosmetic and polymer industries. Aminopyrimidines have for examples been used as nucleic acid base mimics, a base for anticancer drugs e.g. as inhibitors of a subfamily of receptor protein kinases, and in medicinal chemistry as an aniline replacements [18]. During the synthesis of steroids such as Mometasone Furoate (Fig.6) in order to replace the 21-hydroxyl group with a chlorine, sulfonyl chlorides are used in a 4-dimethylaminopyridine (DMAP) base catalyzed sulfonylation reaction [3]. Meta is a glucorticoid that can be used in the treatment of inflammatory diseases.

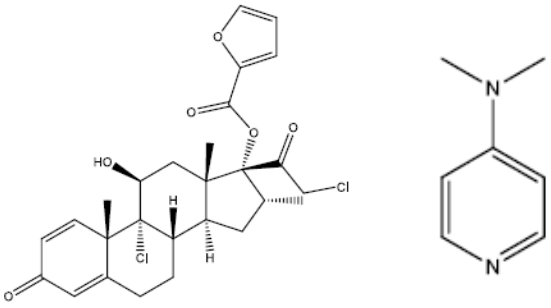

Fig. 5 – Meta (left) and DMAP (right)

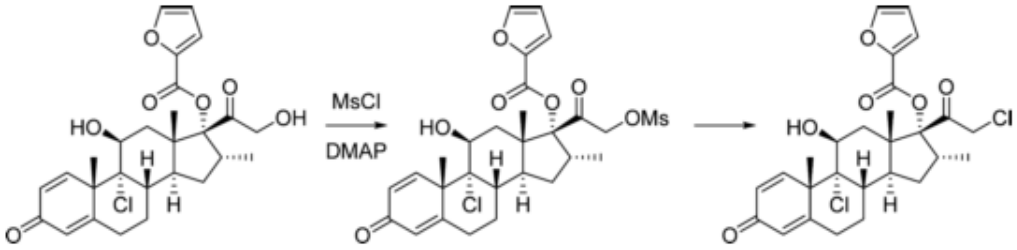

Fig. 6 - DMAP-Catalyzed Sulfonylation during the Synthesis of Mometasone Furoate [2]

1.2- Regulation in pharmaceutical industry

The terms genotoxicity, carcinogenicity and mutagenicity are often misused by chemists. The term genotoxicity refers to a number of genetic damages, regardless of whether or not the damage is corrected through a cellular DNA repair mechanism [2]. A mutagen is able to permanently change part of the genome; such a change is called a mutation that can lead to a change in phenotype. Carcinogenicity may lead to the development of cancer, as it may induce unregulated growth processes in the cells thus leading to the possible development of tumors. [3].

Chirality is a characteristic of almost half of the drugs that are on the market, and in most cases only one of the enantiomers exhibits the desired pharmacologic effect (this enantiomer is called *eutomer*). The inactive enantiomer (called *distomer*) can have no effect, but in some cases it can be an antagonist or it can even be related to toxic effects. The guidelines for the development of new drugs issued by regulating authorities require efficient methods for enantiomeric purity control [19].

There are a number of regulatory authorities and associations, such as the Food and Drug (FDA) [20], European Medicines Agency (EMA), Pharmaceutical Research and Manufacturers of America (PhRMA) [21] and International Council for Harmonization of Technical Requirements for Pharmaceuticals for Human Use (ICH) [22], concerned with safety in pharmaceuticals, thus creating guidelines and standards to control drug development and for manufacturers to know how to deal with genotoxic impurities and chiral purity in pharmaceuticals.

1.2.1- Regulation of chiral drugs

Regulatory authorities guide the development of medicines by providing scientific guidance and regulatory principles. Several regulatory guidelines began to be studied by authorities in many countries in the mid-1980s because of the accessibility of enantiomerically pure drug candidates and the accumulation of knowledge about surgical drugs [23]. In 1992, a Drug Information Association (DIA) workshop on chirality led to discussion on regulatory requirements for chiral drugs [24]. In this workshop, representatives from the pharmaceutical industry from the European Union, Japan and the United States of America debated questions about the quality, safety and efficacy of chiral substances. A regulatory guideline for the development of chiral drugs was first published in the US in 1992 and later in the European Union, adopting the approach advocated at the Drug Information Association (DIA) workshop. The guidelines on active chiral substance investigations were issued by a commission of European countries in 1994 [24]. The Canadian government announced a Therapeutic Product Program to address stereochemical issues in the development of surgical drugs in 2000 [57]. All regulatory orientations emphasize the importance of the chirality of the active ingredient in the bulk drug test, the manufacture of the finished product, the design of stability test protocols and the labeling of the drug. 'It is extremely important that companies evaluate racemates and enantiomers for new drugs and evaluate their behavior. In 2005, the FDA issued a regulatory document reinforcing the importance of the evaluation of the various stereoisomers, the importance of its selection for later commercialization, and the recognition of chirality in new drugs [25].

The FDA states that "in certain situations, the development of an individual enantiomer is particularly desirable ..." [26]. In 1992, the FDA issued a policy statement for the development of new stereomeric drugs, which was later corrected in 1997. The European Communities (EC) Commission formulated a document that provides guidance in the research and development of chiral drugs.

Of the various factors considered, the regulatory agencies emphasize toxicological studies. In a toxicity study, if the toxicity is unexpected, the study with the individual isomers should be repeated to verify that only one enantiomer was responsible for this behavior. Thus, a "favorable" toxicological profile with the racemates supports its development without the need for a separate toxicological evaluation of the enantiomers [26].

1.2.2- Regulation of genotoxic compounds

The Committee for Medicinal Products for Human Use (CHMP) of the European Medicines Agency (EMA) has published a plan of a guideline on the limits of genotoxic impurities and initial US regulatory considerations have been publicly presented [27].

An important regulatory body to issue guidelines is the International Conference on Harmonization of Technical Requirements for the Registration of Pharmaceuticals for Human Use (ICH). The objective of ICH is to promote international harmonization of regulatory requirements; this harmonization avoids the development of duplicate work required for the registration of new medicinal products and their importance in the pharmaceutical industry.

For the development of an ICH guideline there are five steps (Fig.7) which begins with consideration of the topic and development of a consensus by the expert working group (EWG). The resulting EWG project is then released by the ICH steering committee for a wider consultation in the three sponsoring regions. Subsequently, the final guideline is adopted and implemented in the three regions.

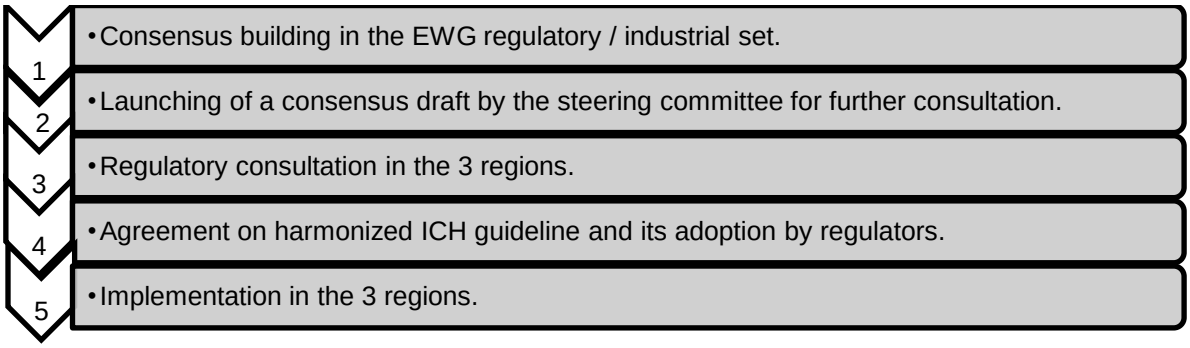

Fig. 7- Scheme of ICH process for the development guidelines based on [18]

The Q3A (R) and Q3B (R) guidelines address issues of impurities in drug substances and pharmaceuticals, respectively. These documents define an impurity as any component of the new drug substance or product that does not have a defined chemical identity. Guidelines Q3C establish acceptable concentration limits or allowable daily exposures for several classes of solvents, but do not define an exposure limitation based on concerns regarding genotoxic potential.

Genotoxic compounds may be carcinogenic to humans because of their ability to induce chromosomal mutations and/or chromosomal rearrangements [28]. In some situations, genotoxic impurities are present in products and pharmaceutical substances, since the ICH guidelines, Q3A and Q3B generally do not require the identification of an impurity until it reaches 0.1% or 1mg/day in a daily dose of a 2g substance or 0.15-1% in the case of a medicament. Currently, the ICH Q3A (R), Q3B (R), and Q3C guidelines focus on issues related to impurities and residual solvents.

In 2004, PhRMA formed a working group to discuss genotoxic impurities that led to the publication of an article by L.Müller, R.Mauthe, C.Riley et al. "The Rationale for Determining, Testing and Controlling Specific Impurities in Pharmaceuticals that Possess Potential for Genotoxicity" [16], which introduced a classification system for genotoxic impurities in five classes (Table 1) that characterize the genotoxic potential of the impurity or establishe permitted specification limits for the impurity in the pharmaceutical product.

The Threshold of Toxicological Concern (TTC) was originally introduced by the FDA Center of Food Safety and Nutrition defines an exposure to an unstudied chemical that does not pose a significant risk for carcinogenicity or other health effect [28]. The stagged TTC is also an essential element in the guidelines of the European Medicines Agency (EMA) and the Food and Drug Administration (FDA).

Table 1 - Classification of genotoxic impurities based on [22]

Class	Description
1	Genotoxic (mutagenic) and carcinogenic impurities.
2	Genotoxic (mutagenic) impurities with unknown carcinogenic potential.
3	Impurities with structural alerts, unrelated to the structure of the API, and with unknown genotoxic (mutagenic) potential.
4	Impurities with API-related alert structures.
5	Impurities without structural alerts or whose absence of genotoxicity is not proven.

EMA has imposed detailed guidelines on how to handle genotoxic impurities. In June 2006, EMA's Committee for Medicinal Products for Human Use (CHMP) published a draft guideline on the limits of impurities, which recommended the dichotomization of genotoxic impurities, that is, a class for impurities in which there is a "sufficient evidence"(experimental) and another class "without sufficient evidence".

The genotoxic impurities with sufficient evidence should be regulated using Q3C guideline methods for class 2 solvents. This approach allows calculating permitted daily exposure (PDE), which is calculated using no observed effect level (NOEL) or lowest observed effect level (LOEL) from animal studies and incorporating a number of uncertainty factors [29].

In the case of impurities without sufficient evidence, the guideline proposes a level control policy "as low as reasonably possible" (ALARP principle). This approach indicates that every effort should be made to prevent the formation of these impurities during drug synthesis and, if this is not possible, post-synthesis efforts should be made to reduce their levels. In cases where genotoxic impurities cannot be avoided, the guideline recommends the implementation of a risk assessment. The standard proposes the use of a "toxicological risk threshold" (TTC, threshold of toxicological concern) for genotoxic impurities.

Table 2 - Allowable daily intake (µg/day) for genotoxic impurities during clinical development using the staged TTC approach [24]

	Duration of exposure				
	Single dose	≤ 1month	≤3months	≤6months	≤ 12months
Daily allowable intake (µg/day)	120	60	20	10	5

In 2008 the Food and Drug Administration (FDA) published a preliminary version of a guide [30] which provides specific recommendations on the safety qualification of impurities with suspected or known carcinogenic or genotoxic potential.

The TTC values established by the FDA for clinical trials are described in Table 3.

Table 3- TTC staged limits proposed by the FDA [25]

	Duration of exposure				
	14 days	>14 Days-1 month	>1-3 Months	>3-6 Months	>6-12 Months
Daily allowable intake (µg)	120	60	20	10	5

1.3- Separation methods

1.3.1- Chiral drugs

The separation of enantiomers is of great interest to the pharmaceutical industry because more than half of pharmaceutically active ingredients are chiral. As mentioned above, chiral compounds exist in two enantiomeric with identical molecular formula but distinct structural arrangement: they are non- superimposable, like an object and its mirror images. Most biomolecules, for example, enzymes, proteins, hormones, nutrients, sugars, fats, and many others are chiral. Usually, only one enantiomer is the active pharmaceutical ingredient. The other enantiomer is often inactive, but it can also be toxic.

Part of the work of this thesis was dedicated to developing processes for the separation of enantiomers. From a pharmaceutical point of view, the potential advantages of single-enantiomer drugs include: separating unwanted pharmacodynamic side effects from toxic effects in case these reside exclusively in one enantiomer, using smaller doses of medication; simpler and more selective pharmacodynamic profile; less complex pharmacokinetic profile; less side-effects because of the elimination of distomers; reduced drug interactions; fewer adverse effects (if one form is more prone to adverse drug interactions)[31].

Currently, separation of racemic mixtures can be performed by the following methods: chromatography, preferential crystallization or stereoselective transformation, enzymatic/chemical kinetic resolution and membrane techniques. Among these chiral separation technologies, membrane processes are perceived as economically and ecologically competitive towards other conventional chiral separation methods. The resolution of enantiomers by membrane separation technology can be done continuously and under mild conditions. The scale-up of the process is relatively easy and, furthermore, it can be regarded as an ultimate energy-saving separation technology. However, the usual commercial membranes, microfiltration, ultrafiltration and nanofiltration membranes do not allow selective separation of individual substances because their separation mechanism only is based on a sieving effect in size dimension. Therefore, the chiral separation cannot be carried out using common separation membranes.

In the last years, methods to develop membranes with controlled specificity for chiral separation have attracted great attention. Various strategies have been adopted such as, for example, introducing chiral selectors into polymer membranes, preparing enantioselective composite membranes, modifying polymer membranes through chiral monomer copolymerization, grafting chiral side chains in the polymer membrane material and designing chiral ligand exchange membranes [32]. Among the membrane-based chiral resolution methods, the development of molecular imprinting technology greatly promotes the design of

novel membranes with specificity for efficient chiral separation. Molecular imprinting is a technique to create polymeric matrices containing tailor-made receptors (sites) with specific molecular recognition ability. When these molecular recognition sites are introduced into polymeric membranes, the obtained product membranes are named molecularly imprinted membranes (MIMs), and now some MIMs have been prepared and used by different researchers to chiral resolution [32].

1.3.1.1- Diastereomeric resolution

The principle of diastereomeric resolution depends on the different physical properties of the diastereomeric salts formed by the complexation of a chiral acidic (or basic) enantiomerically pure resolving agent with each of the enantiomers in the basic (or acidic) racemate, respectively. In this method, the difference in solubility diastereomers salts in the resolution solvent allows the less soluble diastereomeric salt to crystallize while the more soluble remains dissolved [33].

This process can be described in four steps:

1. An acid-base reaction occurs between each of the enantiomer of the racemate and the pure chiral resolving agent.

2. Formation of two diastereomeric salts with different physical or chemical properties (usually solubility)

3. The diastereomeric salts can be separated by crystallization or filtration if one is soluble and the other is insoluble, in the selected resolution solvent.

4. The salt is decomposed by acid or base treatment, yielding the pure enantiomer.

There are many advantages of this process, such as the achievement of high yields and purities. Furthermore, the products are obtained typically in solid form which is convenient for storage and transportation. Besides, this type of process needs relative low capital investments and also allows simple operations.

However, enantioseparation via crystallization is frequently considered as one of the most difficult separation techniques due to the similarity of the two enantiomers. In fact, these enantiomers are identical in almost all physical and chemical properties such as melting point, solubility, nucleation, crystal growth, and reactivity[34].

The initial problem associated with diastereomeric crystallization is selecting the right resolving agent, and the nature and composition of the solvent. This can be time-consuming, tedious and labour-intensive.

A. Przyby and M. Kubicki improved a methodology to extract Lupanine from L. albus followed by diastereomeric resolution with dibenzoyltartaric acids[13]. They obtained (-)-Lupanine by crystallization of racemic mixture of lupanine with (+) - dibenzoyltartaric acid in methanol with an e.e. 99.9% and also (+) - Lupanine by crystallization of racemic mixture of lupanine with (-) - dibenzoyltartaric acid in ethanol with an e.e. 99.9%. Further, from (-) - Lupanine, they obtained (+) –Sparteine.

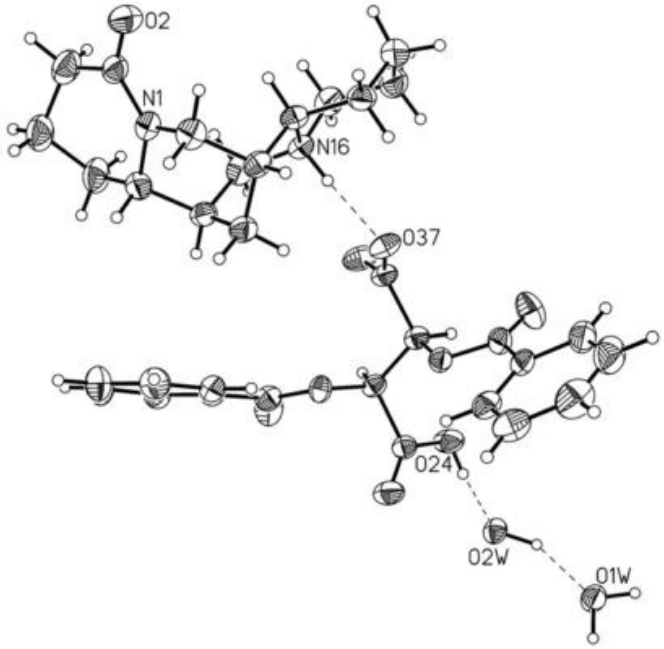

Fig. 8- X-ray of the salt of (-)-lupanine and (+)-2,3-dibenzoyl-D-tartaric acid

It can be seen in figure 8 that lupaninium cation is protonated at the N16 nitrogen atom, and one of the carboxylic groups of the tartrate anion is deprotonated. This was proved by the successful location of these hydrogen atoms as well as by the bond length (carboxylate) and angle (lupaninium) patterns. The crystal structure also contains two water molecules per cation-anion pair. The NH group acts as a donor for a hydrogen bond with the deprotonated carboxylate group and the carboxylic group acts as a donor for a hydrogen bond with the oxygen atom from one of the water molecules. The water molecules are involved in hydrogen bonds with the remaining oxygen atoms.

1.3.1.2- Molecularly imprinted membranes (MIMs)

Molecular imprinting is a methodology offering polymers that feature a molecular memory for molecules present during their preparation [3].

Molecular imprinting is a technique for obtaining custom binding sites, based on the template size and functional groups [35]. The molecularly imprinted polymers (MIPs) are synthesized by copolymerization of the functional monomers and the cross linking agent in the presence of the template. After the removal of the template molecules, binding sites complementary to the template are obtained with size, shape and chemical functionality tailored to highly selectively bind to the target molecules. The MIPs have advantages such as simple synthesis, high stability in adverse chemical and physical conditions and inertness toward organic solvents [36]. There are two main methods to form molecular imprinting, one involves covalent bonds [37] and the other relies on non-covalent interactions between the template molecules and functional monomers [38].

Chiral molecularly imprinted membranes (MIMs) are fabricated by incorporating optically pure print or template molecules into the membranes and then extracting the template molecules to form voids that recognize both the template molecules and the family or analogue of the print molecules. When the racemic solution permeates through the membranes, the print molecules and their analogs are selectively adsorbed to the print sites and the other enantiomers are excluded (Fig.9).

It is also possible to obtain membranes with template specific cavities located in bulk polymer. Such structure governs two mechanisms of selective transport: (i) facilitated transport controlled by preferential sorption and fast diffusion of template molecules, and (ii) retarded permeation caused by affinity binding [39]. In the case of retarded permeation, the transport of the template through the membrane is retarded owing to the binding affinity with the imprinted sites distributed on the surface and bulk structure of the membrane. Basically, this mechanism retains the adsorbed enantiomer in the membrane, while permitting the other enantiomer to pass through the membrane easily since it has no affinity for the chiral recognition sites. In the facilitated transport (typical of micro-porous membranes), the passage of the template through the membrane is quicker and its perm-selective separation is achieved. In this mechanism, one enantiomer preferential adsorbs to the chiral recognition sites in the enantioselective membranes and the other enantiomer, which has no or less specific binding affinity, passes through the membrane by diffusion.

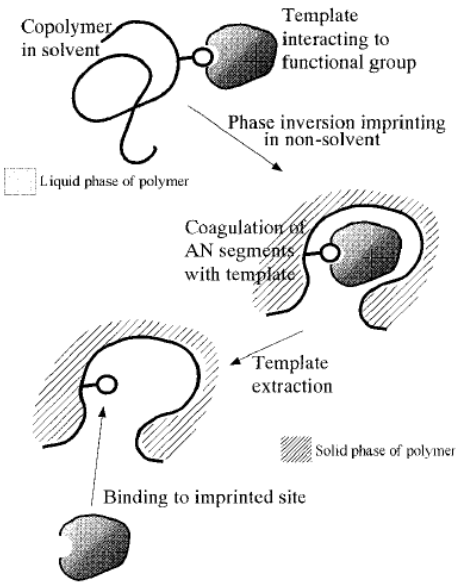

Fig. 9- Scheme of molecular imprinting [35]

MIMs marked a new path for the detection, transport or retention of targeted chemical and biological compounds. Membrane-based imprinting processes do not require additives and can be performed at low temperature, thus reducing the energy consumption costs. In comparison with a traditional membrane, a MIM exhibits an improved specific selectivity maintaining at the same time the separation efficiency [40].

1.3.1.3- Membrane recrystallization

Crystallization is one of the oldest chemical operations to produce, purify or separate the solid products, but only since the 70's it is considered as an unit operation. Nowadays, crystallization and precipitation (solids produced from a chemical reaction) are major processes used in the chemicals, pharmaceuticals, food and electronics industries due the high level of product purity required and the need for low energy requirement. Regardless the crystallizer technology, the crystallization process or the operating conditions, crystallization occurs by a change of the temperature and/or the composition of a saturated solution. Hence, heat and/or mass transfer processes are key issues for the crystallization/precipitation processes [41].

Membrane processes have recently been proposed in order to improve performance of crystallization operations and are considered as one of the most promising strategies. The number of publications dedicated to crystallization / precipitation processes using a membrane have effectively increased in the last years [41].

The ability to couple membrane processes and crystallization operations, in order to develop efficient crystallization technologies, is increasingly reported. The main features of membrane crystallization systems are the ability (1) to control and limit the maximum level of

supersaturation due to defined mass transfer across the membrane; (2) to act as a support able to activate heterogeneous nucleation; (3) to control solid features such as size, shape, polymorphic form, and purity; and (4) to reduce energy consumption. To achieve these goals, several membrane techniques are used: reverse osmosis, membrane distillation, membrane contactor, and membrane templates [42].

A membrane crystallizer is a system in which a solution containing the non volatile solute to be crystallized (defined as the crystallizing solution or feed or retentate) is contacted, by means of a (macro) porous membrane, with a solution on the distillate side. Generally, crystals nucleation and growth in the feed solution is induced by generating supersaturation. This can be done either by removing the solvent from the crystallizing solution, thus increasing solute concentration up to the overcoming of its solubility limit, or by adding an antisolvent to it, which reduces the solubility of the solute in the mixed solvent/antisolvent solution. Accordingly, the role of the membrane is not simply as a sieving barrier to select the transport of specific components, but instead as a physical support which, by removal of the vaporized solvent or by addition of the antisolvent, generates and sustains a controlled supersaturated environment in which crystals can nucleate and grow [43].

1.3.2- “Degenotoxification”

Genotoxic impurities (GTIs) represent a class of compounds of special concern, which can participate in alteration of DNA and subsequently cause cancer.

It should be noted that compounds categorized as GTIs actually include a broad range of unrelated chemicals with very different structures and from very different chemical families. These compounds have in common their ability to react with DNA resulting in an associated carcinogenic risk. However, from a chemical point of view they do not have common chemical-physical properties or chemical structural elements that can contribute to an easy identification. On the other hand, their presence in the manufacture of APIs is not stochastic, since these chemicals often have specific inherent roles in the chemical routes used in API synthesis. The knowledge systematically gathered on GTI formation helped in the assessment of both new and alternative synthetic routes, and allowed scientists to make a more confident decision to embark on purification strategies. Early realization of possible genotoxic contamination of the API improves time lines and safety by avoiding wasted effort on processes with no long-term viability and, in addition, directs the focus to the relevant purification technology [1].

There are different strategies that can be used to reduce GTIs below the limits set by regulatory authorities. One of the strategies is to avoid the use of the genotoxic molecules or precursors in the synthetic route, using different chemical sequences to reach the same API, thus reducing possible interactions with the DNA. Another strategy is to eliminate or reduce the concentration of GTI during the reaction in order to guarantee free GTI drug products. Finally, the API purging of GTIs can be performed directly.

It should be noted that most API purification processes are not GTI specific, but also eliminate other impurities from the raw API. However, the application of eliminators is a selective way of removing a GTI. Generally, the greater the selectivity of purification processes over a specific impurity, the lower the loss of API and the greater the removal efficiency of the impurity in question. However, as other impurities remain in the crude API, the overall purity of the API remains low in relation to all other impurities present.

For the specific removal of GTIs, the selection of the purification method depends on the chemical-physical properties of the compound, such as the reactivity, solubility, volatility and ionizability of the GTI. Some of the conventional purification processes include crystallization, precipitation, extraction, chromatography, treatment with resins and distillation [44]. The efficiency of the separation is based on the differences in the properties of the compounds to be separated and/or their relative affinities for a selective agent. During the last decade other innovative techniques have been developed, such as organic solvent nanofiltration (OSN) and molecularly imprinted polymers (MIPs) [1].

In the field of resins, there are several types of resins with different functional group that removed successfully genotoxic compounds like p-TSA methyl (MTS), ethyl (ETS), and isopropyl (iPTS) esters from APIs [45]. In another study with resins, the researchers removed genotoxic aminopyridine impurities, which are widely used starting materials in the production of pharmaceutical compounds and may potentially be present as genotoxic impurities at trace levels in APIs [46]. With respect to the genotoxic studied in this thesis, the DMAP, it was also developed a study with different resins where were found 3 resins were found with capacity to remove 95% of GTI [15]. Several studies in the field of molecularly imprinted polymers have been explored for the removal of genotoxic impurities. In one of these studies [47], the researchers were able to remove about 98% of DMAP from a Mometasone furoate (Meta) solution.

1.3.2.1- Organic solvent nanofiltration (OSN)

Organic Solvent Nanofiltration (OSN) is a technology that allows size-exclusion based separation of solutes between 50 and 2000 g mol^{-1}, solvent exchange or solvent recovery, all in organic media simply by applying a pressure gradient [48]. OSN relies on separations based mainly on differences in molecule size, where properties like shape and polarity can also contribute. The performance of this technique is highly dependent on the membrane selected and on the respective rejection curve (Fig.10) [3]. The solvent passes through a semi-permeable membrane through the application of pressure.

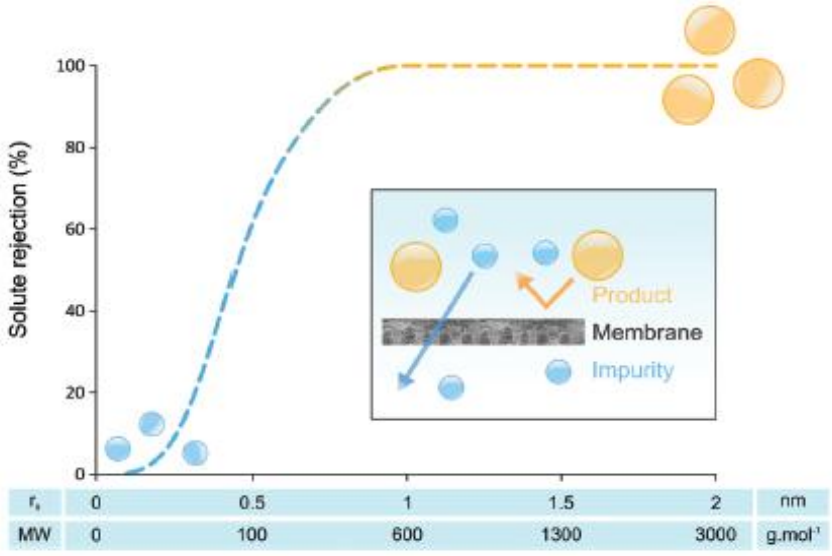

Fig. 10- Basic principle of separation by OSN. Solute rejection plotted against molecular size and weight. The small impurities pass through the OSN membrane, whilst the larger products are retained [38]

N.Hairom et al. developed the dead-end cell system in Fig.11, which consists of a high-pressure filtration cell suitable for nanofiltration and a nitrogen cylinder [49].

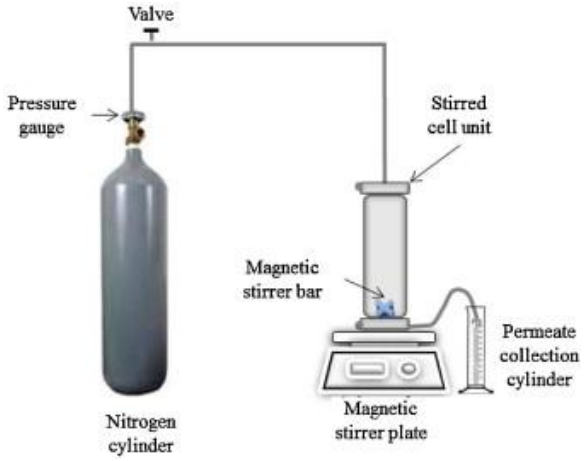

Fig. 11- Filtration cell [49]

Pressure was provided by a nitrogen cylinder and a pressure regulator. The membranes were preconditioned by permeating pure acetonitrile solvent through the membrane until a constant solvent flux was obtained.

Flow rate (Q) is defined in Eq. (2) and it was estimated on the permeate volume (V_{perm}) and filtration time (t).

$$Q = \frac{V_{perm}}{t}\ (Lh^{-1}) \qquad \text{Equation (2)}$$

Solvent flux (J) is defined in Eq. (3) and it was estimated on the basis of membrane area (A_m), permeate volume (V_{perm}) and filtration time (t).

$$J = \frac{V_{perm}}{A_m t}\ (Lm^{-2}h^{-1}) \qquad \text{Equation (3)}$$

Permeability (P) is defined in Eq. (4) and it was estimated on the basis of membrane area (A_m), permeate volume (V_{perm}), filtration time (t) and working pressure (bar).

$$P = \frac{V_{perm}}{A_m t.p}\ (Lm^{-2}h^{-1}bar^{-1}) \qquad \text{Equation (4)}$$

This process is characterized by the rejection of molecules according to the size, charge and shape of the molecule in question. The rejection of the membrane is defined in Eq.(5)

$$R = (1 - \frac{C_p}{C_f}) \times 100$$ Equation (5)

Where C_p is the concentration of permeate and C_f the concentration of feed.

Degenotoxification by OSN mainly relies on the molecular size difference between the API and the GTI, although other properties such as shape and polarity also contribute to their rejection. The aim is to achieve high genotoxin removal through the permeate and low API loss in the retentate. The main challenge of genotoxin removal by membranes lies in the fact that most of them are highly reactive species and thus can attack the polymeric membrane framework at molecular level. Additionally, polymeric membranes are usually prepared by phase inversion in dipolar aprotic solvents such as dimethylformamide and dimethylsulfoxide hence similar harsh solvents can easily attack and dissolve the active layer of the membrane. The performance of this technique is highly dependent on the membrane selected and on the respective rejection curve. There are several commercially available polymeric and ceramic membranes that are stable in organic solvents. Examples include Koch SelRO membranes, StarMem series developed by W. R. Grace & Co, DuraMem series from Evonik MET, SolSep membranes, GMT-oNF-2 from Borsig Membrane Technology GmbH and Inopor or Pervap ceramic membranes. The molecular weight cut off (MWCO) is commonly used to characterize nanofiltration membranes. The MWCO of a given membrane corresponds to the molecular weight of a compound, obtained by interpolation, rejected at 90% [1]. The MWCO value can be determined from rejection of compounds with increasing molecular weights plotted versus the rejection in a MWCO-curve, providing information in which range of solute sizes the membrane is able of molecular discrimination [12].

A continuous purification of the API Roxithromycin from potential genotoxic impurity DMAP has been demonstrated in a simple and efficient two stage membrane cascade where 99% of API could be achieved [50]. In another work, the researchers have been able to successfully proceed to degenotoxification of Mometasone furoate using a commercial membrane GMT-oNF-2, meaning reduction of genotoxics in API post reaction streams corresponding to API related dairy intakes below the recommended TTC value of 1.5 µg day^{-1}. API losses during DMAP removal were 5% and 6.4% for OSN [44].

1.3.3- Freundlich and Langmuir adsorption isotherms and kinetics

The adsorption isotherms allow to describe the phase equilibrium underlying the partition of the solute between the fluid phase and the adsorbed phase. An adsorption isotherm represents the amount of solute adsorbed per amount of adsorbent (qe) as a function of the concentration of the solute at equilibrium (Ce). [51]

Linear isotherms are characteristic of surfaces of very homogeneous adsorbents. Favorable isotherms are quite common. When the surface of the adsorbent is heterogeneous, typically the isotherm is unfavorable. The irreversible isotherm implies that the adsorbent has a high affinity for the solute.

The Langmuir and Freundlich models are the most used to represent isotherms.

The hypotheses underlying the derivation of the Langmuir model are as follows:

1. The surfaces of the adsorbent are homogeneous. all active sites have equal affinity for the solute;

2. There is no interaction between adsorbed molecules;

3. A unimolecular layer of solute molecules is formed;

4. Adsorption is a reversible phenomenon.

The Langmuir isotherm is represented by Equation 1

$$q_e = \frac{q_{max} K_L C_e}{1+(K_L C_e)} \qquad \text{(Equation 1)}$$

q_e represent the amount of solute adsorbed per unit mass of adsorbent (g/g), C_e the equilibrium concentration of solute in solution (g/L), q_{max} the adsorption capacity (g/g) e K_L is a parameter related to the energy of adsorption and that depends on the temperature (L/g). Values of K_L and q_{max} can be obtained by linearization of Equation 1, obtaining Equation 2.

$$\frac{1}{q_e} = \frac{1}{q_{max} K_L C_e} + \frac{1}{q_{max}} \qquad \text{(Equation 2)}$$

Represented $1/q_e$ as a function of $1/C_e$. a straight line with slope $1/ q_{max}K_LC_e$ is obtained and intercept $1/q_{max}$.

The Freundlich isotherm allows to describe the adsorption on heterogeneous surfaces, being represented by Equation 3.

$$q_e = K_F C_e^{1/n} \qquad \text{(Equation 3)}$$

K_F and n are constants. The value of n represents the degree of heterogeneity of the surface, being higher than 1 when the isotherm is favorable and less than 1 when the isotherm is

unfavorable. This model assumes that the adsorbed amount tends to infinity, corresponding to the multilayer formation of adsorbed molecules. As in the previous case, it is possible to linearize the Freundlich equation to determine the K_F and n values.

$$\ln q_e = \ln K_F + \ln \frac{C_e}{n} \quad \text{(Equation 4)}$$

The representation of ln q_e as a function of ln C_e allows to obtain a line with slope 1 / n and intercept ln K_F.

Two types of equations have been commonly used to represent the kinetics. The first one, which corresponds to a diffusion-controlled process, is the intraparticle diffusion equation, together with more elaborate treatments proposed recently. The second one assumes that the process is controlled by the adsorption reaction at the liquid/solid interface in the adsorbent [52]. Two types of kinetics are generally used and compared, namely the pseudo-first order and pseudo-second order rate laws. Pseudo- first order kinetics (hereafter denoted by K1) was first proposed at the end of the 19th century by Lagergren. Pseudo-second order kinetics (denoted by K2) was introduced in the middle of the 80's.

The equation for pseudo-first order kinetics is represented by equation 5

$$\ln(q_f - q_t) = \ln q_f - k_1.t \quad \text{(Equation 5)}$$

q_f represent the amount of adsorbed in equilibrium (g/g), q_t (g/g) it's the amount of adsorbent adsorbed at time t, k1 the pseudo-first order rate constant (h^{-1}) and t the time (h).

Values of K_1 and q_f can be obtained by linearization of Equation 5, obtaining Equation 6

$$q_t = q_f.\left[1 - e^{(-k_1.t)}\right] \quad \text{(Equation 6)}$$

The kinetics of pseudo second order is based on Equation 7 [53]

$$\frac{t}{q_t} = \frac{1}{k_2.q_f^2} + \frac{t}{q_f} \quad \text{(Equation 7)}$$

In which K_2 is the pseudo-second order rate constant (g g^{-1} h^{-1}).

$$q_t = \frac{k_2.q_f^2.t}{1 + q_f.k_2.t} \quad \text{(Equation 8)}$$

Values of K_2 and q_f can be obtained by linearization of Equation 7, obtaining Equation 8

1.4- Polybenzimidazole (PBI) role

Polybenzimidazole (Fig.12) is a thermally stable aromatic heterocyclic polymer that possesses both proton donor (-NH-) and proton acceptor (-N=) hydrogen-bonding sites, which exhibiting specific interactions with both protic and aprotic polar solvents. The availability of hydrogen-bonding sites in the polymer chain makes it a suitable candidate for miscible blending with various polymers possessing carbonyl and sulfonyl functionalities. For example PBI forms a miscible blend in a wider composition range with polyimide, poly(ether imide), and sulfonated polysulfone through the specific interaction of its proton donating (-NH-) site with the proton accepting sites of the other polymers. PBI is being used for various applications, in particular, for high temperature applications, fiber spinning, and reverse osmosis membranes, because of its excellent thermal-chemical tolerance and film forming capability [54].

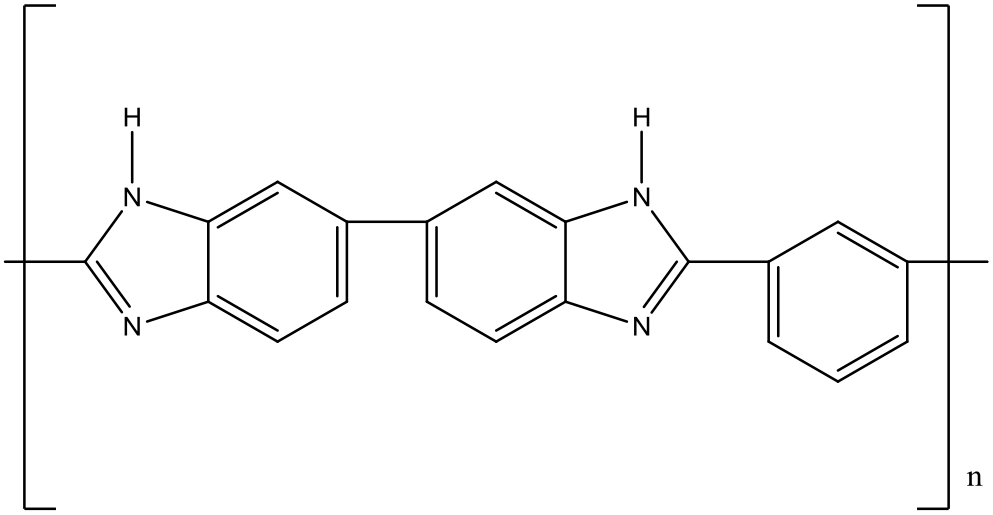

Fig. 12- Polybenzimidazole (PBI)

PBIs have been reported in the literature since the early 1960s. However, in the last few years work at Hoechst Celanese has demonstrated that (i) PBI can be made at high molecular weight, (ii) PBI is moldable and (iii) advantage can be taken from PBI's solubility in dimethylacetamide (DMAc) allowing for the facile preparation of PBI matrix resin composites containing continuous fiber reinforcement. PBI is hydrophilic. PBI has a Tg of about 420-435 ºC*;* as a result, its mechanical properties remain quite stable up to 100 ºC [55]. In the 1980s and 1990s, many new PBI microporous membranes were developed to broaden PBI applications. For example, microporous resin beads were invented for liquid chromatographic separation.

More recently PBI has gained much attention for applications in gas separation, aqueous nanofiltration (NF), forward osmosis and fuel cells due to its outstanding properties (thermal,

mechanical and chemical stability in corrosive environments). In addition, PBI has the advantage of possessing excellent stability towards acids and bases [56].

Reactions for the synthesis of APIs are essentially carried out in organic solvent and thus, the interest in producing and studying new materials relevant to the production process of APIs that are suitable to be used in the same type of solvents. Following this, PBI is a very interesting polymer because it is compatible with organic solvents.

Functionalization of PBI for the removal of genotoxic impurities can be performed through the following the patent application submitted by our group [57].

2- Materials and Methods

2.1- Materials, equipments and analytical methods

The racemic Lupanine was kindly provided by Professor Carlos Afonso (Faculty of Pharmacy of the University of Lisbon). Di-*p*-toluoyl-L-tartaric acid was purchased from Acros organic, Di-*p*-toluoyl-D-tartaric acid and L-tartaric acid were purchased from Alfa Aesar. Sodium Sulfate (Na_2SO_4) was purchased from Fluka. Hydroxide Potassium (KOH) and Hydroxide Sodium (NaOH) was purchased from Panreac. Dibromo-*p*-xylene (DBX) were purchased from Fluka. Acetonitrile (MeCN), Isopropanol (IPA), Acetone, Dichloromethane (DCM), Hexane and Methanol (MeOH) was purchased from Fisher Scientific. Silica Gel 60 was purchased from MERCK. Polypropylene non-woven was purchased by NOVATEX. Polystyrene 580 (PS 580) was purchased from Agilent Technologies (Germany) and Coomassie Brilliant Blue R250 was purchased from Fluka.

4-Dimethylaminopyridine (DMAP) was purchased from Acros. Polybenzimidazole (PBI) polymer 100 mesh powder and 26 wt% PBI solution in dimethylacetamide standard dope solution were purchased from PBI Performance Products Inc. (USA). Mometasone furoate (Meta) was kindly provided by Hovione PharmaScience Ltd (Portugal). Formic acid (FA) and Dimethylacetamide (DMAc) was purchased from Panreac (Spain).

The Rotavapor used was Rotavapor R-3 BUCHI.

Nanofiltration experiments were performed on HP4750 Stirred Cell from STERLITECH.

The concentrations of Lupanine were determined on HPLC (Labchrom) with a Kinetex 5µm EVO C18 100Å LC column (250mm x 4.6mm) using a L-7100 pump, D-7000 Interface Module, L-7250 Autosampler and L-7400 UV detector (λ=220 nm), where the mobile phase consisting of 15% of MeCN and 85% of aqueous Na_2HPO_4 solution (pH 10.5) at a flow rate of 1mL/min and 24 min of run time.

The enantiomeric excess of Lupanine was measured at the Faculty of Pharmacy of the University of Lisbon in a SHIMADZU HPLC with a CHIRALPAK IC column (250mm x 4.6mm). This equipment uses a LC-20AT pump and a SPD-M20A Diode array detector. The mobile phase consisted of 55.0% of hexane, 22.0% of IPA and 25.0% of hexane with 0.1% of diethylamine at a flow rate of 1mL/min and 45 min of run time.

The concentrations of DTTA were determined on a Merck Hitachi pump coupled to a L-2400 UV detector (λ=259 nm) and L-2200 Autosampler using a Nucleosil 10µm C18 100Å LC column (250mm x 4.6mm) with a flow rate of 0.5 mL/min. For these analyses, a solvent gradient was

employed from water to MeCN solution in 20 min, followed by a plateau of 5 min for the MeCN solution and between 25-30min a solvent gradient from MeCN to water.

The concentrations of DMAP and Meta were determined on a Merck Hitachi pump coupled to a L-2400 UV detector (λ=259 nm) and L-2200 Autosampler using a Nucleosil 10µm C18 100 Å LC column (250mm x 4.6mm) with an injection volume of 10 µL; eluents, A: aqueous 0.1% FA solution, B: MeCN 0.1% FA solution. UV detection at 280 nm and a flow rate of 1 mL/min For these analyses, a solvent gradient was employed with the method: 0-3 min, 60%-20% A; 3-4 min, 20% A; 4-8 min, 20%-60% A; 8-15 min 60% A.

The concentration of tartaric acid was determined on a Hitachi pump coupled to a L-2420 UV-Vis detector (λ= 210nm) and L-2200 Autosampler using a Rezex ROA column (300mm x 7.8mm) at 65ºC with a flow rate of 0.5 mL/min. For these analyses, the mobile phase is 50mM H_2SO_4 in H_2O.

2.2- Methods

2.2.1- Lupanine extraction

3.5L of the residual water collected in a lupin mill/processing plant (Phase 3) was basified with NaOH to a pH above 12 in order to neutralize the lupanine. Lupanine was then extracted two times with 2.5 L of MTBE. After phase separation, the collected organic phases were dried over anhydrous sodium sulfate, filtered and evaporated to dryness in a rotary evaporator. For purification, the extracted lupanine was dissolved in the minimum amount of hot hexane and left to recrystallize at room temperature for 1-2 days.

2.2.2- Polybenzimidazole treatment

- **PBI-COOH**

For the functionalization of the PBI with carboxylic acid groups (-COOH), 0.5g of PBI polymer was dissolved in 3.13 mL of 1,4 dimethylsulfoxide (DMSO) and the solution was stirred for 3 hours under reflux. The solution was cooled to 50 ° C and 0.4405 g of K_2CO_3 were added. The solution was allowed to stir approximately 10 minutes in order to deprotonate the PBI. After this time, 3-bromopropionic acid (1 equivalent) was added and allowed to react under reflux and stirring for 24h at 100ºC. Finally, the reaction was cooled to 50 ° C and water was added to precipitate the polymer; the solid was triturated and left under stirring for a few minutes; and then it was filtered and washed with water, MeOH and DCM. The brown solid obtained was dried under vacuum.

The reaction scheme of the synthesis is shown in Fig. 13.

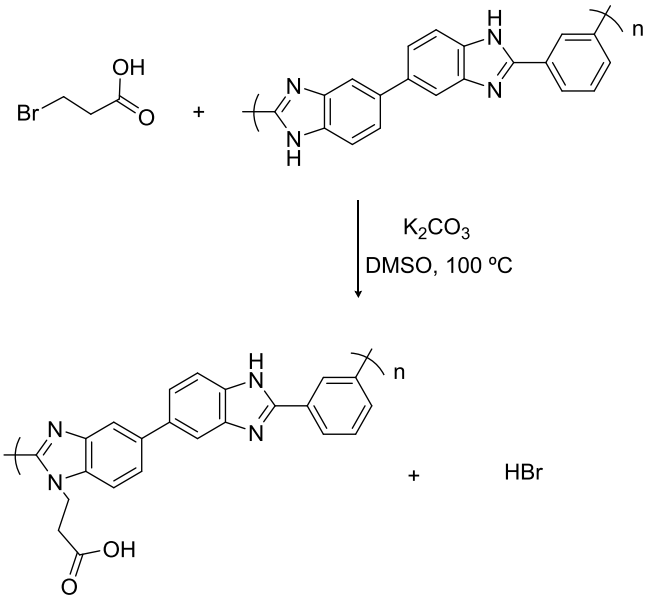

Fig. 13 - Reaction scheme of the synthesis of PBI modified with 3-bromopropionic acid

- PBI-T (thermal treatment)

PBI raw polymer was dissolved in DMSO (15% w/w) by refluxing for 3 h with magnetic stirring. The solution was cooled to 50 °C for 10 min, and then heated at 100 ºC for 24 h and cooled again to 50 °C. The polymer was precipitated with water, and the resulting solid was crushed, filtered and successively washed with water (40 mL/g polymer), MeOH (20 mL/g polymer) and DCM (20 mL/g polymer) for 3 min with magnetic stirring (3 times for each solvent). The solid obtained was then dried under vacuum.

- PBI-TA (acid treatment) and PBI-TB (basic treatment)

For pH conditioning PBI thermal was pH conditioned with HCl 0.25 M or NaOH 0.1 M solutions by washing, with 20 mL of acidic or basic solution per g of polymer, for 3 min with magnetic stirring. After this, the polymer was successively washed with water (40 mL/g polymer), MeOH (20 mL/g polymer) and DCM (20 mL/g polymer) for 3 min with magnetic stirring (3 times for each solvent) and dried under vacuum overnight.

2.2.3- Binding tests

2.2.3.1- Binding of Lupanine to PBI

The experiments to determine the binding of lupanine to the polymer were perfomed as follows:

• 50 mg of PBI, 1 mL of lupanine solution in H_2O, DCM and MeCN (1 g/L) and a small magnetic stirrer were added to an Eppendorf tube of 2 mL, which was then placed in a stir plate at 200 rpm for 24 hours at room temperature.

• the Eppendorf tube was centrifuged at 11000 rpm for 5 minutes;

• finally, the supernatant solution was separated from the pellet, filtered with a syringe filter and further analyzed in HPLC to quantify the lupanine.

Protocol for the preparation of the sample for HPLC analysis:

In order to measure the lupanine concentration after the binding experiment, the sample were basified, (with KOH), until a pH 13, and then centrifuged and filtered. For the solutions prepared in DCM and MeCN, the solvent had to be evaporated. For that, the samples were left in the hotte for two days, bubbled with N_2, and ressuspended in 1mL of water. After that, the same procedure of basification, centrifugation, and filtration was performed previous to the injection of these sample in the HPLC.

2.2.3.2- DMAP and Meta mixtures

The experiments to determine the binding of DMAP and Meta to the polymer were perfomed as follows:

• 50 mg of PBI, 1 mL of DMAP in DCM (1000 ppm) and a magnetic stirrer were added to an Eppendorf tube of 2 mL, which was then placed in a stir plate at 200 rpm for 24 hours at room temperature; the same experiment was performed for Meta (10000 ppm) and for DMAP+Meta (1000 ppm and 10000 ppm, respectively).

• the Eppendorf tube was centrifuged at 11000 rpm for 5 minutes;

• finally, the supernatant solution was separate from the pellet, filtered with a syringe filter and further analyzed in HPLC to quantify the DMAP and Meta;

2.2.5- Molecularly imprinted membrane

2.2.5.1- Molecularly imprinted membrane manufacturing and pos treatment

The matrix used was from Polybenzimidazole (PBI) which is a thermally stable high performance polymer. The reactions for the synthesis of pharmaceutical compounds are usually carried out in organic solvent and, hence, the interest in developing new materials that are compatible with the same type of solvents. We employed PBI because this polymer is compatible with organic solvents like N-Methyl-2-pyrrolidone (NMP), Dimethylacetamide (DMAc) and Dimethylformamide (DMF).

Polybenzimidazole membranes with lupanine imprinted were prepared by phase inversion technique following the figure 15.

Fig. 14- Process of phase inversion for membrane fabrication

The commercial available 26 wt% PBI dope solution was diluted to 21% in DMAc and use as:

i. 21wt% PBI solution for preparation of non-imprinted membrane (NIM)
ii. 21wt% PBI solution + 5 wt% (with regards to the polymer) of template for preparation of imprinted membrane (MIM)

This solution was left under mechanical stirring at 50 rpm overnight in order to homogenize the solution. Aluminum foil was used to protect the dope solution from light and the solution was allowed to stand for 24 hours to remove bubbles. This solution was then cast on the polypropylene non-woven support using a bench top laboratory casting machine (Elcometer) with a casting knife of 250 µm at a temperature of 25-27ºC and a humidity of 40-50%. Dimethylacetamide (DMAc) and water were selected as the casting solvent for the polymer and the coagulation medium, respectively. After the cast, the membranes were washed twice with distilled water (1h+1h) in the coagulation bath and then placed in a bath containing isopropanol for about 30 minutes (twice).

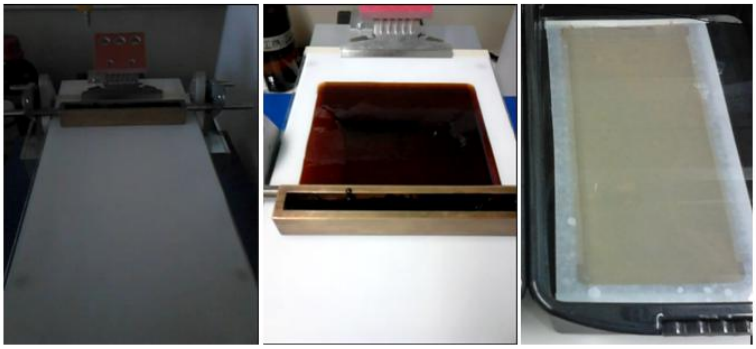

a) b) c)

Fig.15 - a) Adjust of casting knife above polypropylene non-woven support; b) Cast of membrane; c) Coagulation bath

The previous membranes were cut in 3 pieces: the first was used as control, the second was cross-linked with a solution of 3wt% of DBX in 100mL of MeCN and third was cross-linked with a solution of 3wt% of DBX in 100mL of MeCN + 1g of lupanine. The cross-link reaction was carried out at 80ºC for 24h under constant stirring and reflux. After cross-linking, the membranes were first immersed in IPA to remove residual reagents.

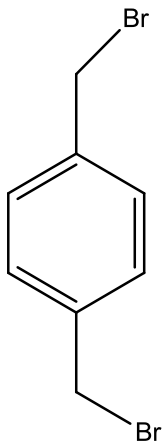

Fig. 16- Dibromo-p-xylene (DBX)

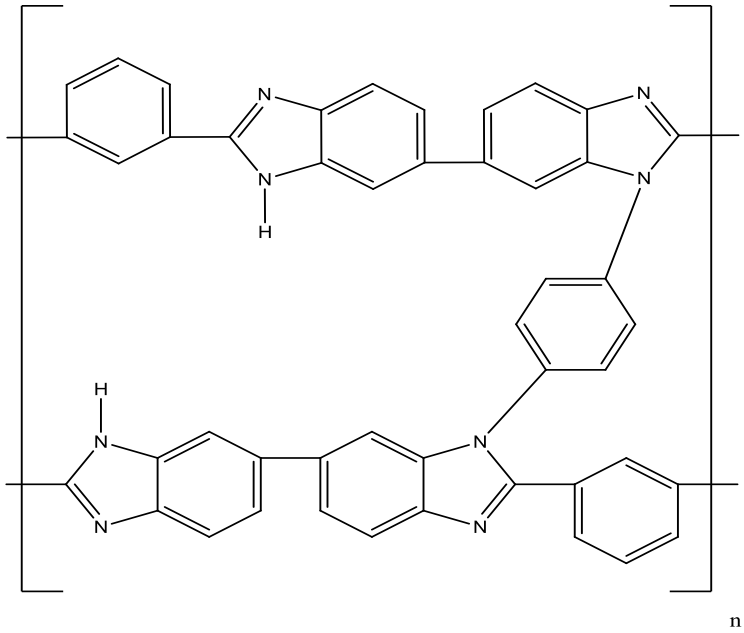

Fig. 17- Scheme of cross-linked PBI with DBX

2.2.5.2- Membrane adsorber

The membranes used as membrane adsorber were prepared initially with the same procedure described in chapter 2.2.5.1. After casting, the membranes were placed in a coagulation bath of distilled water for 1 h, then placed in solutions of HCl (0.25 M) or NaOH (0.1 M) for about 3 minutes after is again placed in distilled water for 1h and then placed in a bath containing isopropanol for about 1h (twice).

The membrane with a area of 0.0012 m^2 was placed in a falcon with 7 mL of DMAP and Meta solution in DCM with a concentration of 1000 ppm and 10 000 ppm respectively, where it was left for 24h under stirring of 200 rpm.

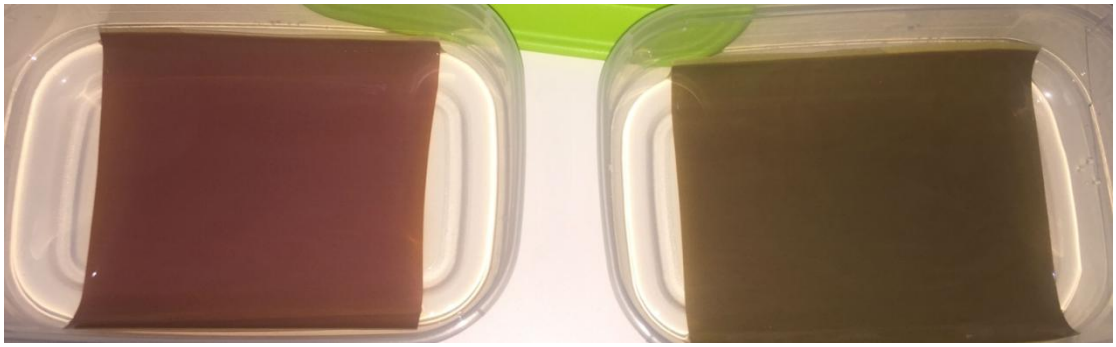

Fig.18- Membrane with HCl bath (right) and NaOH (left)

2.2.5.3- Nanofiltration

The membranes prepared in the previous section (2.2.5.1) were used in nanofiltration to register the rejection and flux of the different membranes. The membranes were preconditioned by permeating pure acetonitrile solvent through the membrane until a constant solvent flux was obtained and for that, 200 mL feed solution was placed in the feed tank.

150mL was filtered and recovered as well as the 50mL of retentate was also recovered for analyze. Subsequently, 200 mL of pure MeCN was replaced, 150mL filtered and it was analyze the 300mL of permeate and 100mL of retentate to check if the template (lupanine) was removed.

50 mL of a solution of lupanine in acetonitrile (1g/L) was passed through the membrane to quantify the rejection percentage of the membrane. As a final step we washed the membrane twice with 200mL of MeCN, in order to remo ve the lupanine trapped in the membrane.

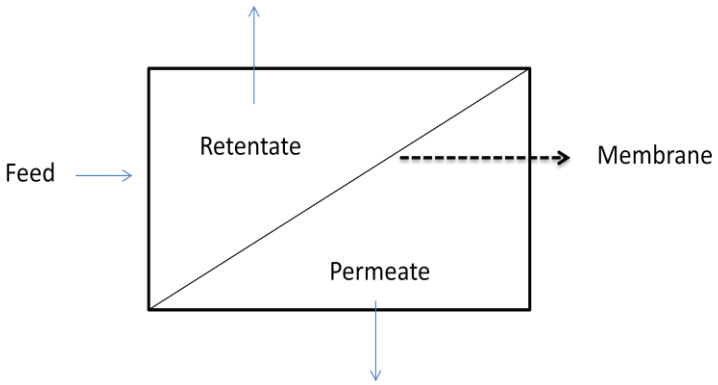

Fig. 19- Scheme of process of OSN

2.2.6- Diastereomeric resolution

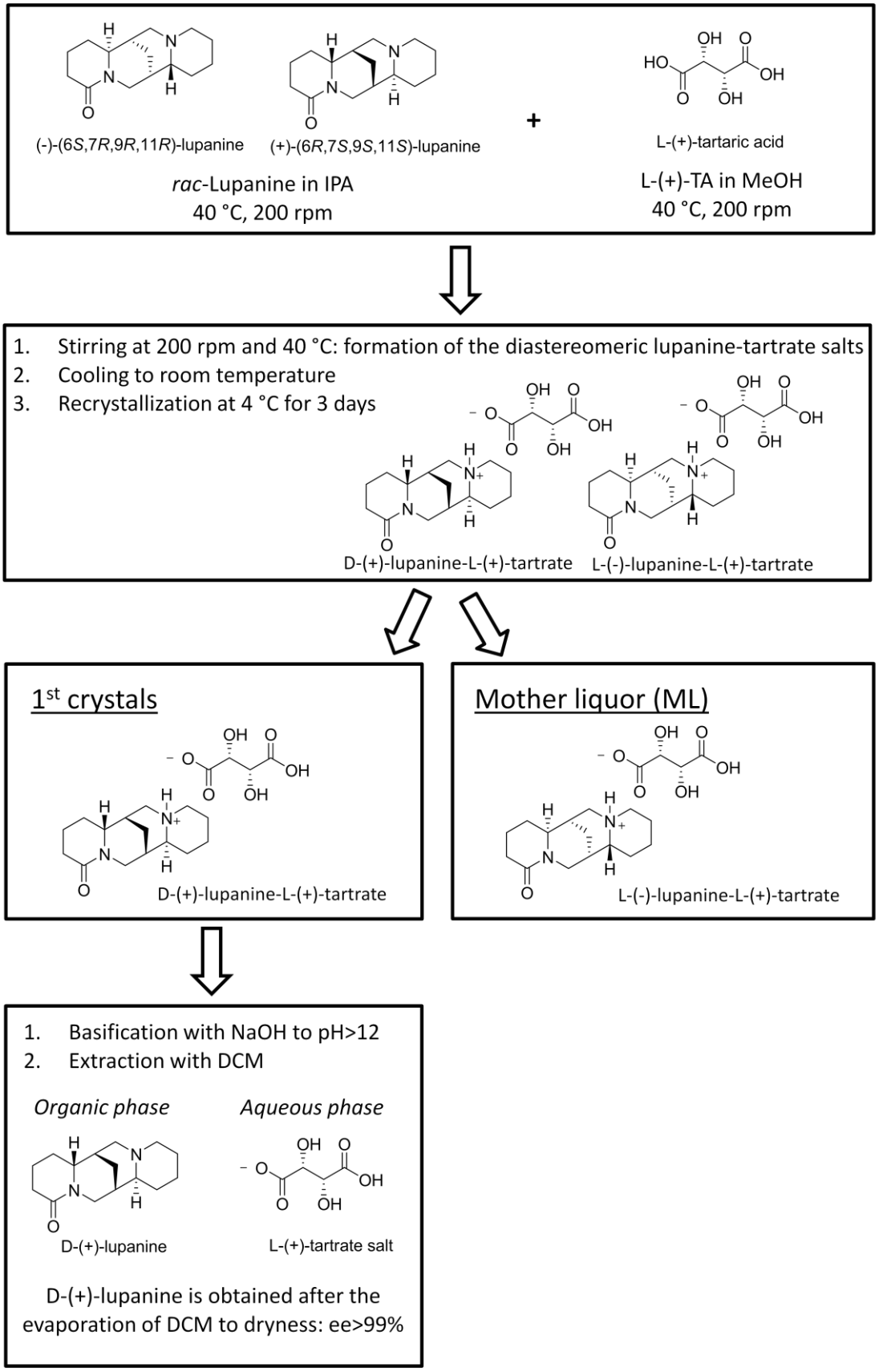

The general procedure for diastereomeric resolution consists in dissolving the racemic lupanine and the resolving agent (DTTA,TA), separately, in hot solvent and then mixing both solutions and leave to cool to room temperature. After that, the samples are left to recrystallize in the fridge.

After 2-3 days, the mother liquor was separate from the crystals obtained and placed again in the fridge to allow the remaining compound to recrystallize (after the first crystallization, the other enantiomer is in excess and starts recrystallizing together with the chiral acid). The crystals formed are a salt of cationic lupanine (either its D or the L enantiomer) and the resolving agent used, in its anionic form.

The crystals recovered after each crystallization step are washed with acetone, dried and then weighed to measure the yield of the recrystallization. After that, they are dissolved in approximately 20 mL of aqueous NaOH (1M) to neutralize the corresponding enantiomer. This leads to the deprotonation of the amine which has been protonated by the resolving agent, rendering it neutral and making possible its extraction from the solution with an organic solvent such as dichloromethane (DCM). The resolving agent is in the aqueous phase. The aqueous phase is extracted two times with 20ml of DCM. The organic phases are collected, dried over anhydrous sodium sulfate, filtered and evaporated to dryness in the rotavapor. The samples to be injected in the chiral HPLC (for quantification of the enantiomeric excess, e.e) were re-dissolved in DCM and passed through a Pasteur pipette with silica, to ensure the high purity of the samples injected in the chiral column. After evaporating the DCM to dryness, 2 mg of the lupanine were dissolved in 100 µL of IPA (HPLC grade), to which 900 µL of hexane (HPLC grade) were added.

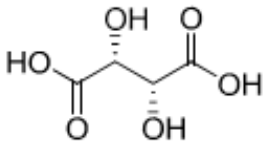

Fig. 20- L-tartaric acid; Mw= 150.09 g/mol

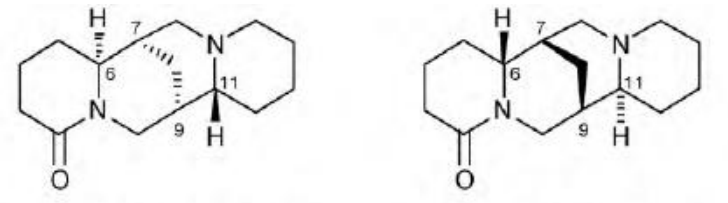

Fig. 21 -(+)- Lupanine and (-)- Lupanine; Mw=248.36 g/mol

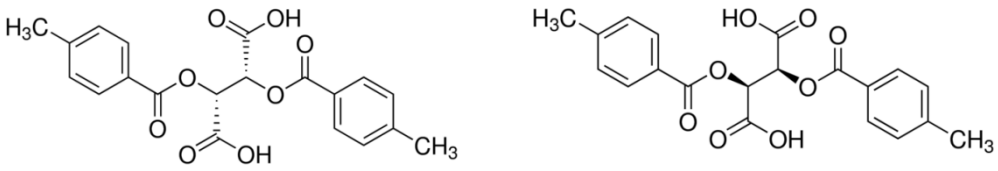

Fig. 22- Di-p-toluoyl-L-tartaric acid and Di-p-toluoyl-D-tartaric acid; Mw= 386.35 g/mol

To calculate the enantiomeric excess of each experiment the following formula as employed:

$$e.e\ (\%) = \frac{Area\ D(+) - Area\ L(-)}{Area\ D(+) + Area\ L(-)}$$

To calculate the yield of each experiment the following formula was employed:

$$\eta\ (\%) = \frac{mass\ of\ enantiomer\ isolated\ from\ the\ crystallization}{initial\ mass\ of\ Lupanine} \times 100$$

3- Results and discussion

3.1- PBI as scavenger

3.1.1- Lupanine

In order to assess the PBI with higher lupanine binding in different solvents: H_2O, dichloromethane and acetonitrile with different PBIs were studied:

- PBI-Raw: PBI pristine
- PBI-T: PBI raw polymer with thermal treatment
- PBI-TA: PBI-T with acid treatment
- PBI-TB: PBI-T with basic treatment
- PBI-COOH (3C): PBI functionalized with carboxylic acid groups.

Two parallel experiments with two different concentrations, a concentration of 3 g/L, were carried out due to the fact that a phase 3 (wastewater that is recovered during the debittering process of the lupin beans) is most often with this concentration value and concentration of 1 g/L, due to the fact that most of experiences are to perform to this standard concentration.

Table 4 - Binding of Lupanine

	% Binding Lupanine						
	1g/L			3g/L			
	H_2O	DCM	MeCN	Phase 3	H_2O	DCM	MeCN
PBI-RAW	5.86 ± 1.50	2.3 ± 0.24	14.61 ± 2.95	19.92 ± 5.33	9.81 ± 1.72	16.45 ± 4.17	15.15 ± 0.45
PBI-T	20.76 ± 5.8	88.07 ± 3.7	54.86 ± 6.56	16.72 ± 9.08	45.76 ± 10.91	25.77 ± 9.76	55.26 ± 1.42
PBI-TA	31.55 ± 6.33	**93.62 ± 0.56**	**85.63 ± 1.96**	20.33 ± 7.81	24.0 ± 2.61	**72.3 ± 12.99**	**74.56 ± 1.84**
PBI-TB	**82.64 ± 2.65**	53.72 ± 10.20	66.39 ± 5.57	22.99 ± 1.99	42.36 ± 6.17	9.23 ± 1.18	55.85 ± 6.96
PBI-COOH (3C)	**>99.81**	49.21 ± 10.60	**92.66 ± 5.84**	40.81 ± 17.27	**99.85 ± 0.07**	68.8 ± 21.04	**95.63 ± 1.75**

At a concentration of 1 g/L in water, it can be observed that there is more binding with PBI-TB and PBI-COOH which may be due to the functional groups that these types of PBI contain; also for a 3g/L concentration, there is high binding of lupanine in water with PBI-COOH (3C). In the case of dichloromethane, the best result is observed with the PBI-TA that due to its acid composition ends up by better grasping the lupanine whereas in the case of acetonitrile the best binding is observed with the PBI-COOH where a hydrogen bond or even a covalent bond between the amine group (R-NH) of lupanine and the carboxylic group (R-COOH).

Regarding phase 3, the best result was with PBI-COOH. We can see in figure 32 that there may be an ionic interaction between the anionic carboxylate group of PBI-COOH and the protonated Lupanine nitrogen present in phase 3. Comparing phase 3 with Lupanine in water to a concentration of 3 g / L, there are better binding results with respect to the second, which may be due to the fact that phase 3 is not only lupanine but also in its constitution other macromolecules. In this case, a better binding in PBI-COOH is also observed.

Table 5- Possible chemical interactions between PBI-COOH and PBI-TA with lupanine (see annex 3)

	Lupanine
PBI-TA	• Hydrogen bond between PBI-TA amine and lupanine nitrogen. • The double bond of oxygen of lupanine can form a hydrogen bond with the amine of the PBI
PBI-COOH	• The double bond of oxygen can form a hydrogen bond with the amine of PBI • The carboxylic group may form a hydrogen bond with the lupanine nitrogen • If lupanine is protonated in lupanine nitrogen and deprotonated PBI-COOH, it may have an ionic interaction.

An experiment was carried out in which the pH of phase 3 was adjusted with NaOH (1M) to 10. There was a significant increase binding of lupanine with phase 3 being the basic pH. For this we used the PBI-COOH since it was the best result in terms of binding with phase 3 where the binding was of 40.81%; with phase 3 with pH adjust for 10, the result was 89.35%, that is, when lupanine is in its neutral form it has better binding, which can be verified with the value of binding vs lupanine in water represented in table 9.

Finally, we use the above-mentioned experience along with two other best binding's to see if we can do the regeneration of PBI.

After the binding's, the supernatant was removed and PBI was allowed to dry and then 1mL of dichloromethane was added to the polymer leaving 24h under stirring at 200rpm.

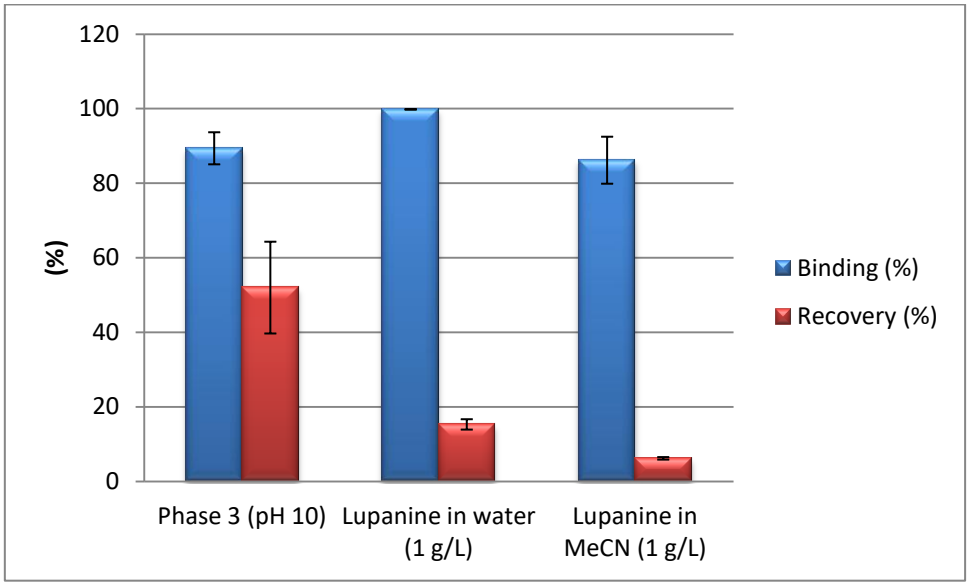

Fig. 23- Regeneration of PBI with DCM

As can be seen in figure 23, dichloromethane was not efficient in the regeneration of PBI. It is necessary, in future works, to strengthen and deepen the regeneration of PBI trying to find the best solvent to use. The use of alcohols such as methanol or ethanol may be a possibility as they break down hydrogen bonds that form during binding as well as exploit the use of NaOH or HCl to regenerate the PBI in order to break down previously formed ionic interactions.

3.1.1.1- Adsorption isotherms and kinetics

To obtain the adsorption isotherms, solutions of lupanine at concentrations of 0.25. 0.75. 1.5. 2. 2.5. 3 and 4 g/L were prepared and 50 mg of PBI-COOH was added to 1 ml of Lupanine solution in water. The solutions were stirred for 24 hours at 200 rpm at room temperature and the concentration of Lupanine in solution was then determined.

The adsorption isotherms allow to describe the phase equilibrium underlying the partition of the solute between the fluid phase and the adsorbed phase. To trace an adsorption isotherm, the amount of solute adsorbed by amount of adsorbent is plotted as a function of the concentration of the solute in equilibrium.

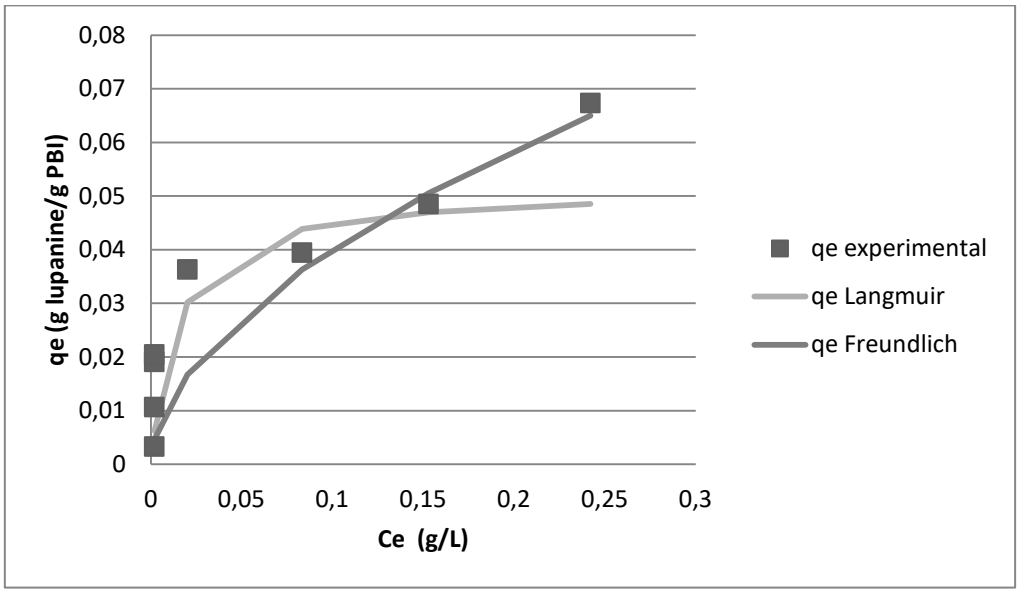

Fig. 24 - Adsorption isotherm for binding of PBI-COOH with Lupanine in water

It was verified that initially the isotherm of PBI-COOH with lupanine in water follows the Langmuir model and then tends to follow the Freundlich model, however, the most suitable model to represent this isotherm is Langmuir.

To obtain the kinetics, a solution of lupanine in water with a concentration of 1g/L was prepared and 0.5 mg of PBI-COOH was added to 1 ml of this solution. The solutions were stirred for 24 hours at 200 rpm at room temperature and samples were taken at 0.25, 0.5, 0.75, 2, 4, 8, 24 and 27 hours and the amount of Lupanine adsorbed was then determined.

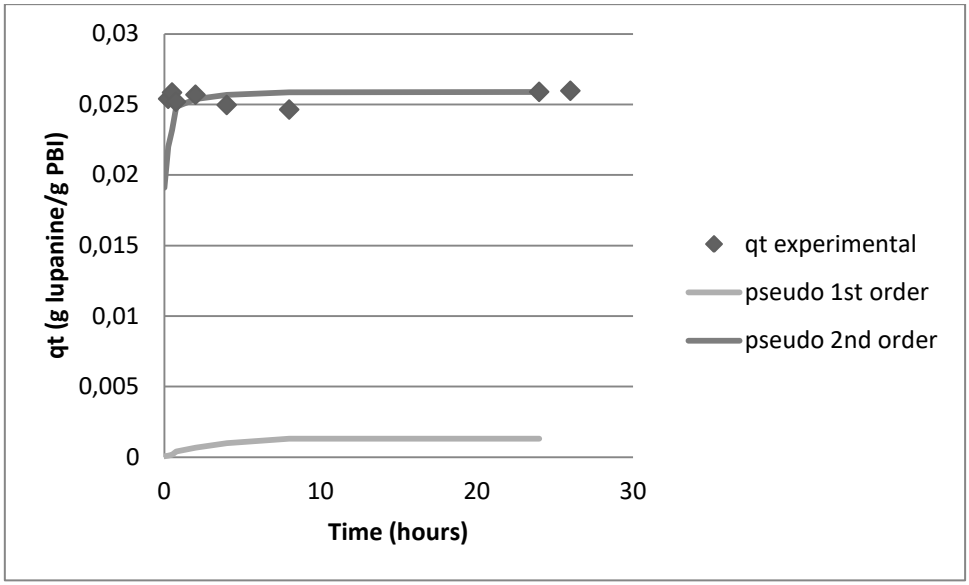

Fig. 25- Adsorption kinetics for binding of PBI-COOH with Lupanine in water

It was verified that the adsorption kinetics of PBI-COOH with lupanine in water follows the pseudo 2nd order.

3.1.2- DMAP and Meta mixtures

Table 6 - Binding of DMAP and Meta

Binding (%)				
	DMAP	Meta	DMAP+Meta	
Initial concentration	1000 ppm	10000 ppm	1000 ppm+10000 ppm	
			DMAP	Meta
Raw PBI	2.88 ± 1.85	6.07 ± 0.34	3.13 ± 0.61	12.39 ± 0.15
PBI-T	78.90 ± 0.49	4.24 ± 3.47	77.34 ± 0.01	14.52 ± 0.53
PBI-TA	**> 99.95**	1.62 ± 0.32	**98.55 ± 0.16**	**6.82 ± 5.88**
PBI-TB	**93.55 ± 0.03**	8.90 ± 3.39	55.78 ± 3.41	12.5 ± 4.42
PBI-COOH (3C)	**95.77 ± 0.24**	3.92 ± 3.85	**91.6 ± 0.97**	**6.17 ± 4.53**

The best results are relative to the PBI-TA and PBI-COOH (3C) where an almost 100% DMAP adsorption and a low adsorption of Meta, which is the objective of our work, is verified.

Relative to the Meta molecule, low binding values can be caused by stereochemical impediment, thus making it difficult to bind the PBI to Meta due to the shape of its molecule. As can be seen in figure 41, the Meta molecule does not have many sites where it binds to the PBI, most likely it may be the formation of a hydrogen bond of the -OH group or a hydrogen bond of the oxygen double bond as shown in the figure. Access to the -OH group should be hampered by the geometry of the molecule.

.

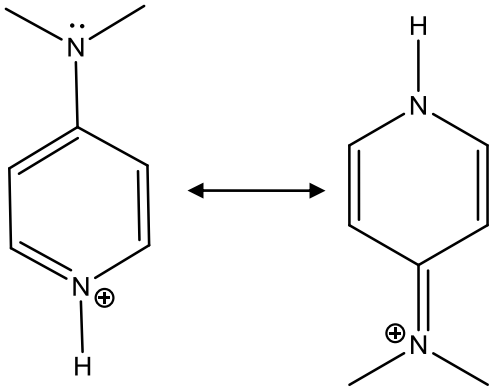

Fig. 26- Two forms of equilibrium for the protonated DMAP

In the case of PBI-COOH and PBI-TB there is an ionic interaction with the COO- of the PBI and the protonated nitrogen of the DMAP. The DMAP may have two different protonation conformations in acid medium depicted in Fig. 26.

Table 7- Possible chemical interactions between PBI-TA, PBI-TB and PBI-COOH with DMAP

	DMAP
PBI-TA	• Hydrogen bond between PBI-TA amine and DMAP nitrogen.
PBI-TB	• Ionic interaction between the protonated amine of DMAP and deprotonated amine of PBI-TB
PBI-COOH	• Ionic interaction between the protonated amine of DMAP and deprotonated carboxylic acid of PBI-COOH • In the case, where the carboxylic group is not deprotonated and when the DMAP is not protonated, a hydrogen bond may be formed between amine of PBI and nitrogen of DMAP.

After the binding's, the supernatant was removed and PBI was allowed to dry and then 1mL of MeOH was added to the polymer leaving 24h under stirring at 200rpm. The same procedure was performed with DCM.

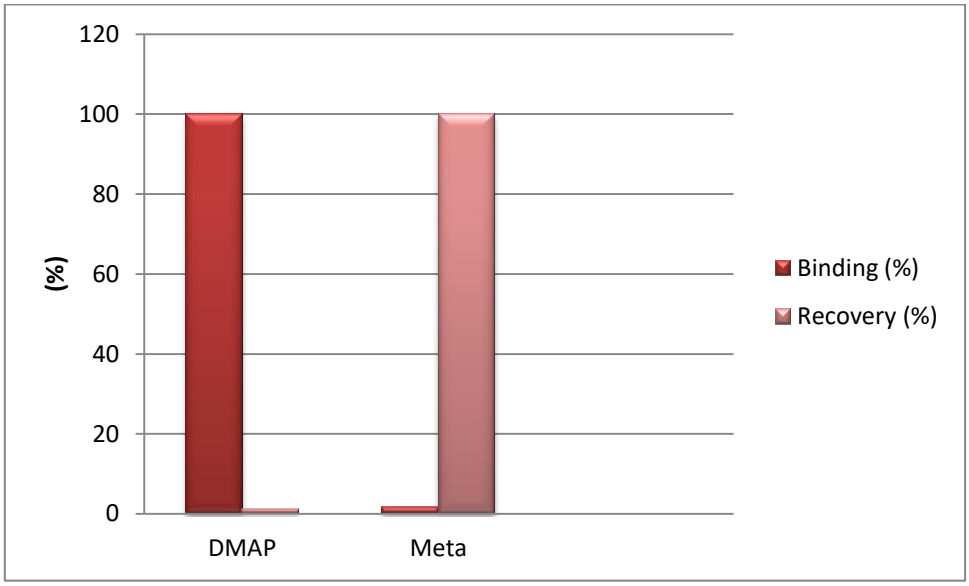

Fig. 27- Regeneration of PBI with DCM

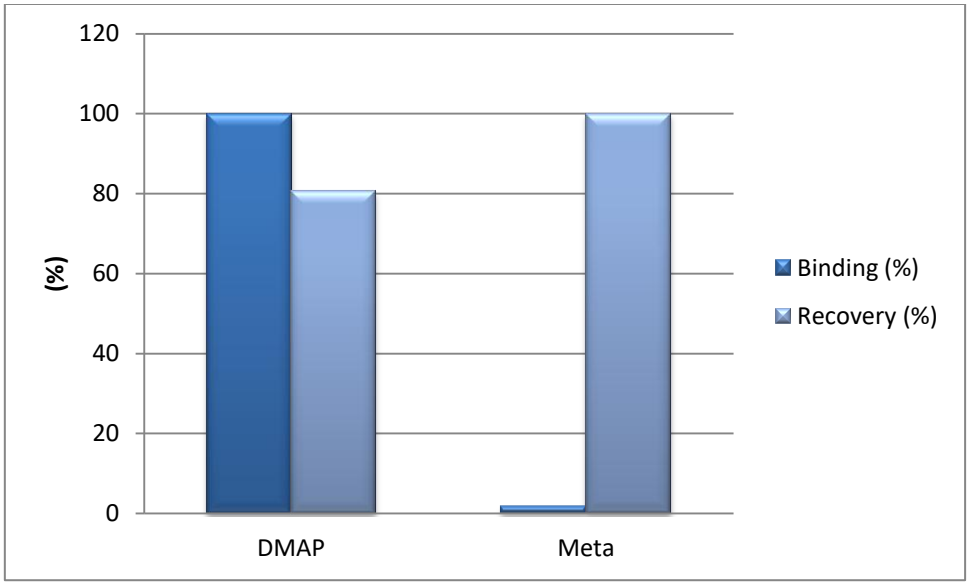

Fig. 28- Regeneration of PBI with MeOH

As can be seen in figure 27 and 28, dichloromethane was not efficient in the regeneration of PBI in the case of DMAP but with MeOH only about 20% of DMAP remained in PBI. In the case of Meta, both DCM and MeOH result for the total recovery of Meta and complete regeneration of PBI.

3.1.2.1- Adsorption isotherms and kinetics

To obtain the adsorption isotherms, solutions of DMAP at concentrations 100, 500, 1000, 2000, 3000, 4000 and 5000 ppm were prepared and 50 mg of PBI-TA was added to 1 ml of DMAP solution in DCM. The solutions were stirred for 24 hours at 200 rpm at room temperature and the concentration of DMAP in solution was then determined.

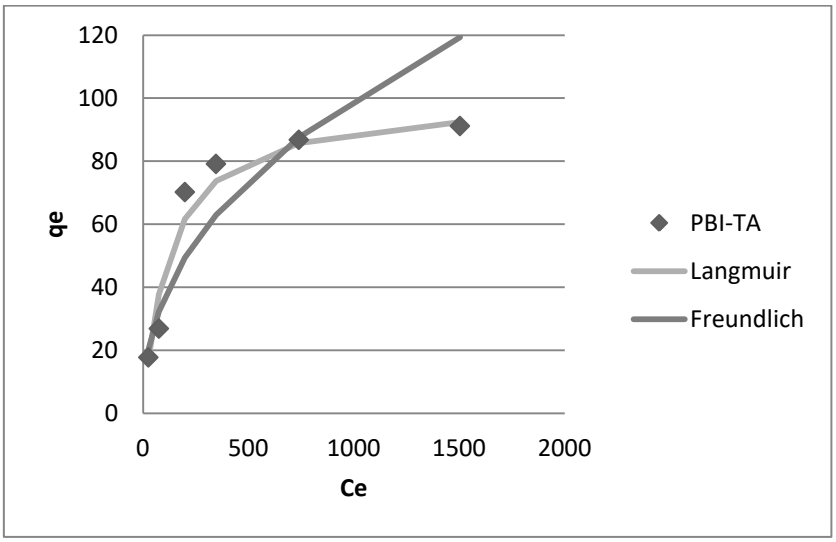

Fig. 29- Adsorption isotherm for binding of PBI-TA with DMAP in DCM

It was verified that initially the isotherm of PBI-TA with DMAP in DCM follows the Langmuir model so, the most suitable model to represent this isotherm is Langmuir.

To obtain the kinetics, a solution of DMAP in DCM with a concentration of 1000 ppm was prepared and 50 mg of PBI-TA was added to 1 ml of this solution. The solutions were stirred for 24 hours at 200 rpm at room temperature and samples were taken at 0.25, 0.5, 0.75, 1, 2, 4, 6, 8 and 27 hours and the amount of DMAP adsorbed was then determined.

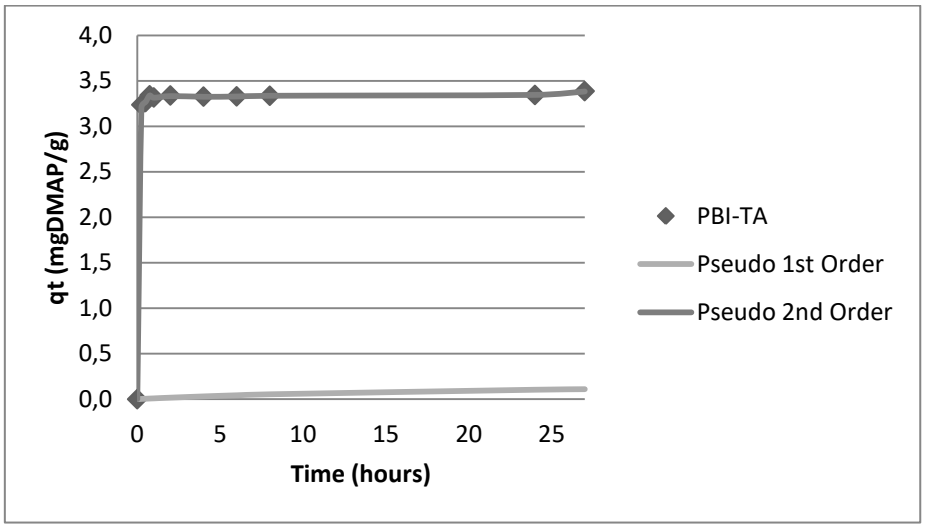

Fig. 30- Adsorption kinetics for binding of PBI-TA with DMAP in DCM

It was verified that the adsorption kinetics of PBI-TA with DMAP in DCM follows the pseudo 2nd order.

To obtain the adsorption isotherms, solutions of Meta at concentrations 100, 500, 1000, 2000, 5000 and 10000 ppm were prepared and 50 mg of PBI-TA was added to 1 ml of Meta solution in DCM. The solutions were stirred for 24 hours at 200 rpm at room temperature and the concentration of Meta in solution was then determined.

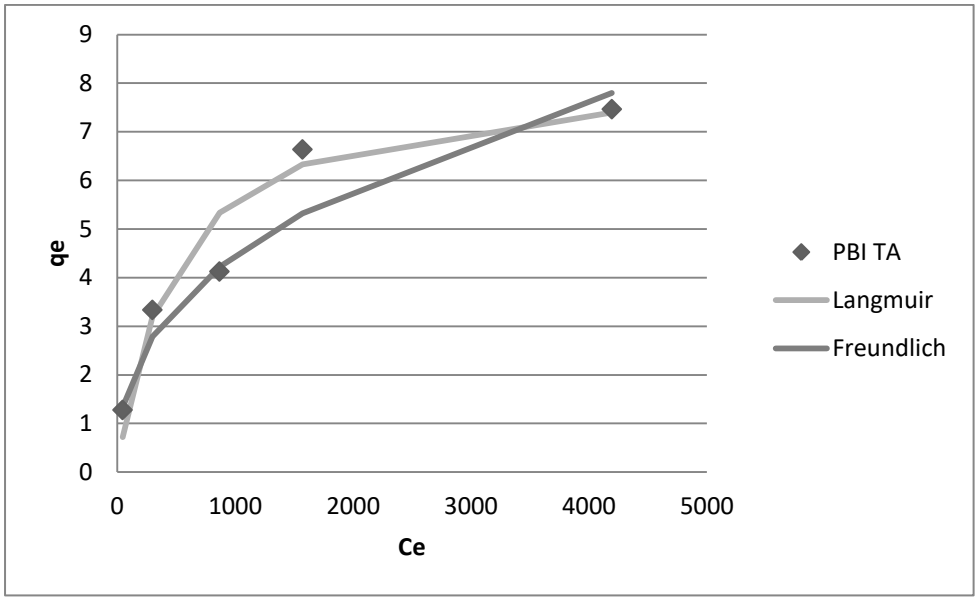

Fig. 31- Adsorption isotherm for binding of PBI-TA with Meta in DCM

It was verified that initially the isotherm of PBI-TA with Meta in DCM follows the Langmuir model so, the most suitable model to represent this isotherm is Langmuir.

3.2- PBI membranes adsorbers

3.2.1- Lupanine

In this section three different membranes were tested:

i. NIM: non-imprinted membrane
ii. MIM L-(-)- Lupanine: imprinted membrane with L-(-)-Lupanine as template
iii. MIM: imprinted membrane with racemic lupanine as template

For each membranes was carried out two type of x-link:

- X-link with a solution of 3wt% of DBX in MeCN
- X-link with a solution of 3wt% of DBX in MeCN+1g of racemic lupanine

In this experiment a membrane area of 52.56mm^2 was used in contact with a solution of Lupanine in MeCN (1g/L) for 24h under stirring of 200rpm.

Adsorption tests were performed using the non-imprinted and imprinted membranes in order to verify if these membranes have Lupanine adsorption capacity and their potential used as membrane adsorber.

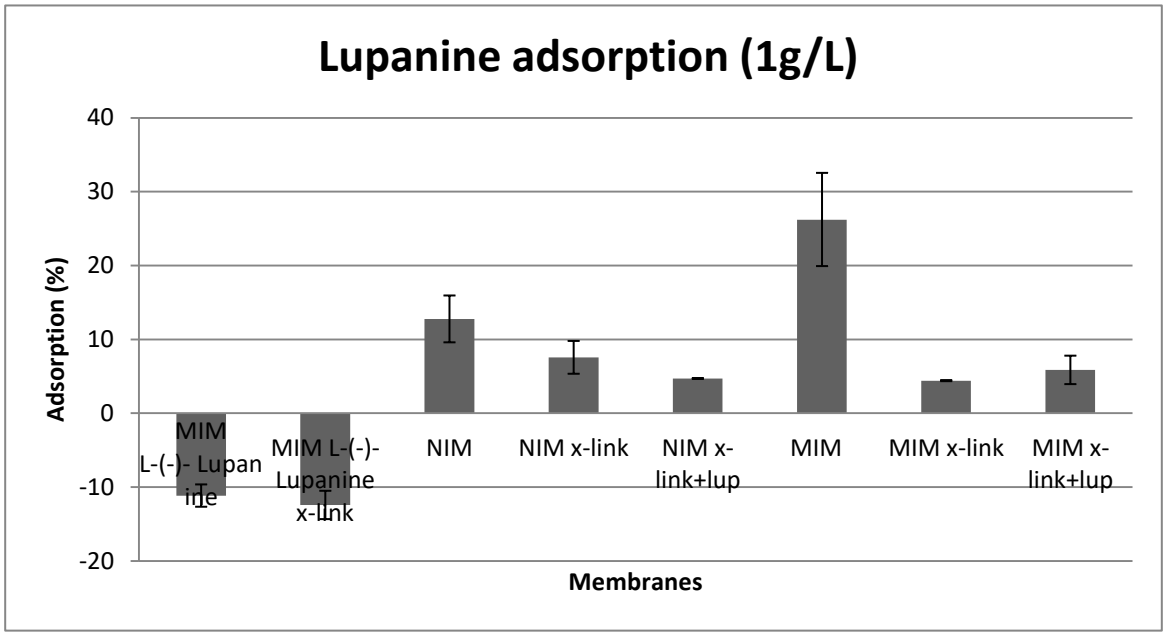

Fig. 32- Lupanine adsorption with PBI membranes

Figure 32 shows that the MIM has a higher adsorption percentage compared to NIM, i.e., manufacturing the membrane in the presence of the template increases the adsorption capacity. As far as non imprinted and imprinted membranes are concerned, the x-link of the membrane decreases the capacity to adsorb lupanine, which may be due to decrease in surface area or charge induced in the membrane. Regarding the membranes containing the enantiomer L-Lupanine there was a negative adsorption, possibly part of the template left in the membrane matrix was washed out during this adsorption process.

3.2.2- DMAP and Meta mixtures

Table 8- Quantities of GTI and API adsorb by the membranes and percentage of adsorption

		g/m^2	**Adsorption (%)**
Meta	PBI-TA	7.95 ± 0.64	10.99 ± 0.88
	PBI-TB	7.76 ± 0.55	10.73 ± 0.73
	PBI-T	0.95 ± 0.08	0.87 ± 0.11
DMAP	PBI-TA	3.58 ± 0.2	67.36 ± 3.77
	PBI-TB	0.62 ± 0.01	11.74 ± 0.76
	PBI-T	1.32 ± 0.05	24.87 ± 1.32

By observing the adsorption of Meta by the membranes, it is verified that the PBI-TA and PBI-TB membrane has a similar adsorption, i.e., the fact that the membrane receives an acid and basic bath increases the affinity with the Meta molecule that is the opposite of what is intended.

Regarding the adsorption of DMAP, the only reasonable result is reached with the PBI-TA while values of low adsorption are observed with the PBI-TB and with PBI-T.

As can be seen in the table above, non-imprinted membranes with both acid bath and basic bath have low adsorption for both DMAP and Meta. The only good result is the 0.87% Meta adsorption with the PBI-T membrane, since the goal is to remove the GTI from the API so a low percentage of API removed is ideal. With this, it can be concluded that the use of these membranes is not a good option for our purpose.

3.2.3- PBI beads vs PBI membranes for DMAP and Meta

Table 9- Comparison between beads and membranes

	g de PBI/mL of solution		Adsorption DMAP (%)		Adsorption Meta (%)	
	Membranes	Beads	Membranes	Beads	Membranes	Beads
PBI-TA	0.013	0.051	67.36 ± 3.77	98.55 ± 0.16	10.99 ± 0.88	6.82 ± 5.88
PBI-TB	0.010	0.051	11.74 ± 3.77	55.78 ± 3.41	10.73 ± 0.73	12.5 ± 4.42
PBI-T	0.011	0.050	24.87 ± 1.32	77.34 ± 0.01	0.87 ± 0.11	14.52 ± 0.53

The amount of PBI per ml of solution used is about 5 fold lower with PBI membranes than with beads. However, the percentage of adsorption is lower.

With this, another experiment was performed with the beads of PBI and with the same mass of PBI per mL of solution to verify if the adsorption results are concordant.

Table 10- Comparison between beads and membranes for the same mass of PBI

	g de PBI/mL of solution		Adsorption DMAP (%)		Adsorption Meta (%)	
	Membranes	Beads	Membranes	Beads	Membranes	Beads
PBI-TA	0.013	0.010	67.36 ± 3.77	66.24 ± 0.84	10.99 ± 0.88	8.15 ± 2.77
PBI-TB	0.01	0.011	11.74 ± 0.76	19.92 ± 5.58	10.73 ± 0.73	6.08 ± 4.82
PBI-T	0.011	0.011	24.87 ± 1.32	36.56 ± 6.37	0.87 ± 0.11	14.07 ± 6.84

As can be seen in the table above, we can see that when using approximately the same amount of PBI, the adsorption values are similar, especially the values that refer to DMAP. The goal is to purify the API (Meta) by removing the GTI (DMAP) and with the beads we get a lot more GTI than the API. In the experiment shown in Table 11, with beads of PBI-TA, we were able to remove 98.55% of DMAP while only 6.82% of Meta is adsorbed, thus being able to remove the genotoxic only with 50mg of adsorbent (in this case, PBI). However, the ideal would be not to adsorb any API.

3.3- Nanofiltration with PBI membranes

The molecular weight cut off (MWCO) is commonly used to characterize nanofiltration membranes. The MWCO of a given membrane corresponds to the molecular weight of a compound, obtained by interpolation, rejected at 90%. Two different compounds, brilliant blue (792.85 g/mol) and polystyrene 580 (580 g/mol) were used to define the MWCO of two types of membranes, non-imprinted (NIM) and imprinted membranes (MIM).

The membrane was placed in filtration cell and conditioned with pure acetonitrile and a solution of PS and AB in acetonitrile (1 g/L) was filtered to record rejection of each. This procedure was performed for each compound, separately.

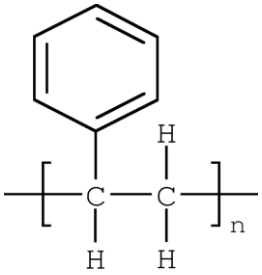

Fig. 33 - Polystyrene

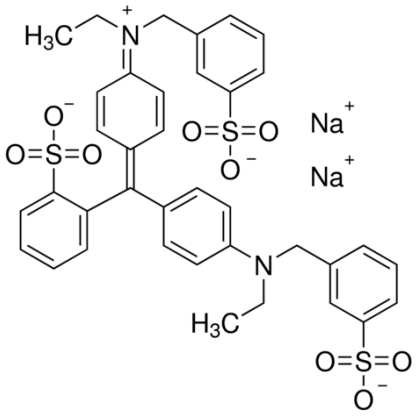

Fig. 34- Brilliant Blue

.

Table 11 - Rejection value of Brilliant Blue and PS 580 in MeCN

	MIM	NIM
Rejection of Brilliant Blue (%) **Mw=792.85 g/mol**	99.38	98.1
Rejection of Polystyrene (%) **Mw=580 g/mol**	68.54	92.13

The table above demonstrates the percentage of rejection of each compound and with these rejection values we were able to determine the cut off value of each membrane.

Taking into account the rejection values, we can conclude that the MWCO of the non-imprinted membrane (NIM) is below 580 g/mol and the MIM is between 580 g/mol and 792.85 g/mol.

In this section three different membranes were tested:

iv. NIM: non-imprinted membrane
v. MIM L-(-)- Lupanine: imprinted membrane with L-(-)-Lupanine as template
vi. MIM: imprinted membrane with racemic lupanine as template

For each membrane two type of x-link were performed:

i. X-link with a solution of 3wt% of DBX in MeCN
ii. X-link also with a solution of 3wt% of DBX in MeCN but with 1g of racemic lupanine. This type of x-link was performed in an attempt to promote a concentration driving force that avoids leaching by diffusion of the template from the polymer matrix to solution during the x-link process (T(ºC)=80; DBX reaction)

Each membrane was placed in filtration cell and conditioned first with pure acetonitrile and after that a solution Lupanine in MeCN (1 g/L) was filtered to record rejection of each type of membrane.

The figure 33 shows the purpose of this experience, i.e., separate the enantiomers of lupanine. For that, it was placed one enantiomer of lupanine as template. When the filtration of the racemic material is carried out, one of the enantiomers stays in the membrane and the other one passes to the permeate.

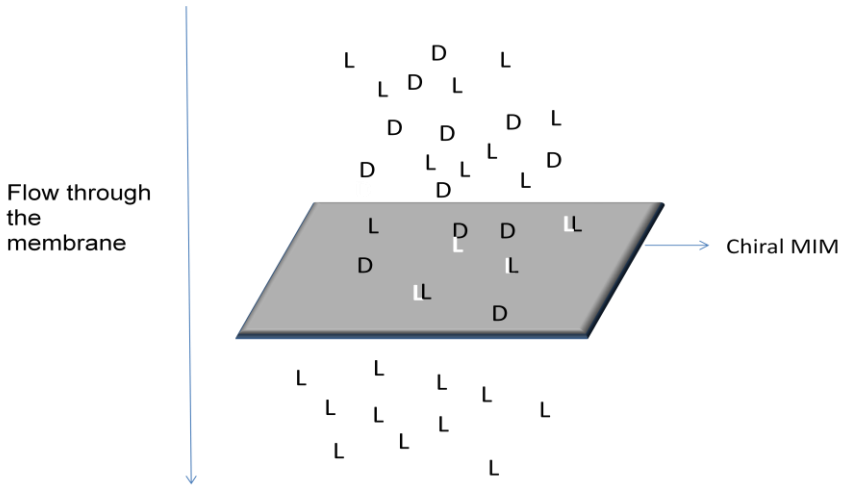

Fig. 35- Purpose of a chiral MIM

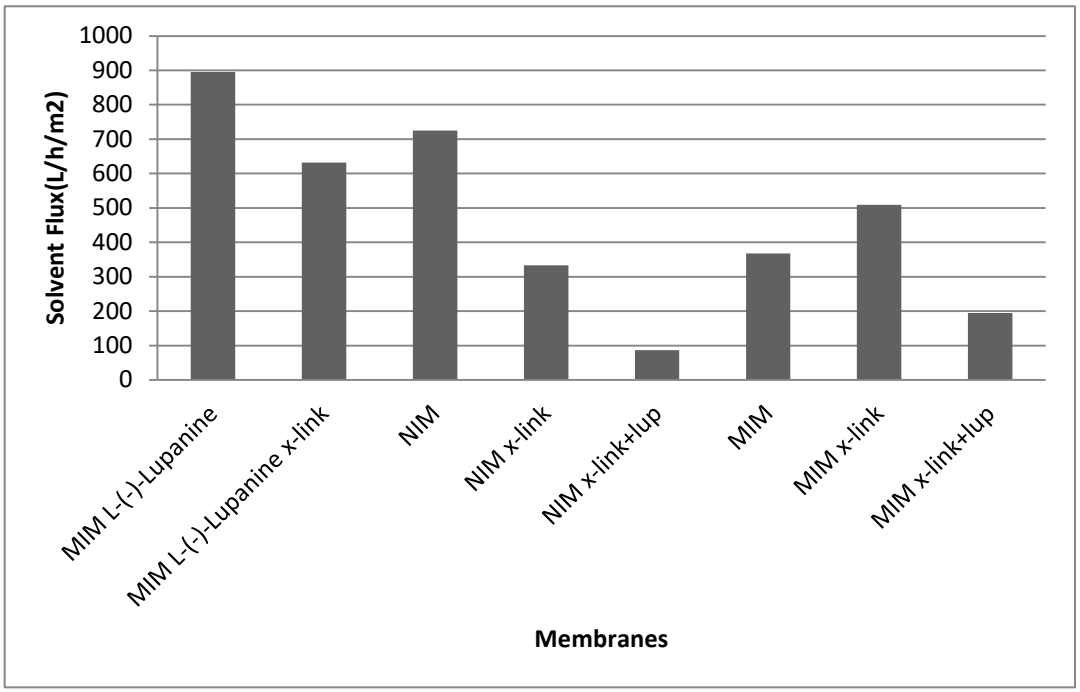

Fig. 36- Flux performance of the imprinted and control membranes measured in acetonitrile at 20 bar

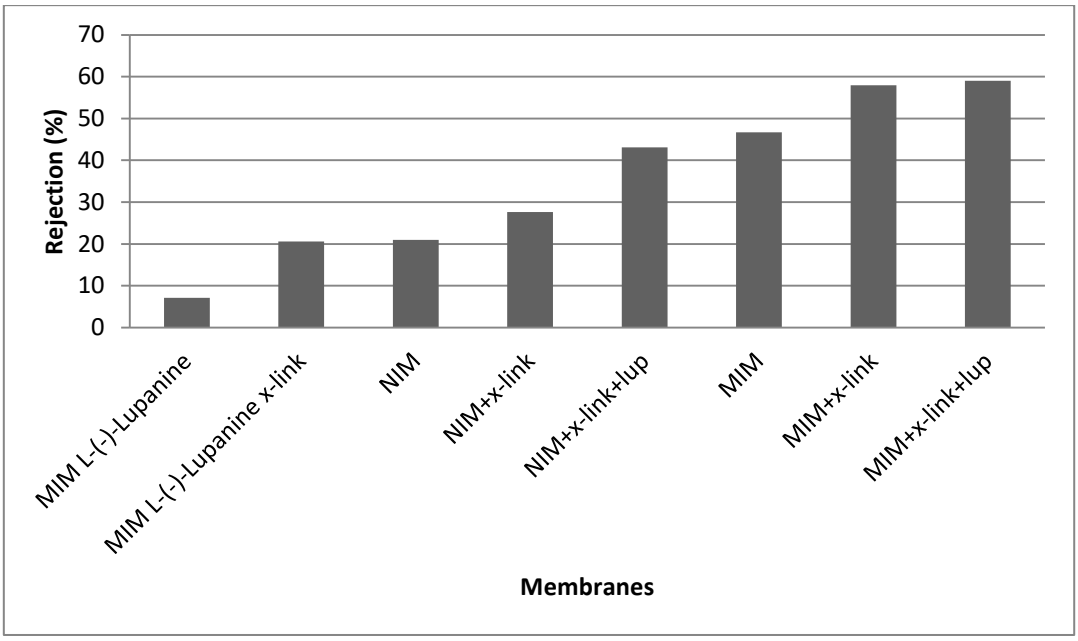

Fig. 37 - Rejection of the imprinted and control membranes measured in acetonitrile at 20 bar.

Observing the Figures 34 and 35, it is important to focus on 3 different points:

1. X-link: while the rejection increases, the solvent flow decreases because pores between polymer chains are smaller. With respect to the solvent flux In the non-imprinted membranes, the results show decrease flow with x-link as more closed/tight membrane with small pores is obtained. The same trend is observed for membranes prepared using as template the pure lupanine; however for membranes prepared using racemic lupanine as template this trend is no longer observed.
2. X-link+lupanine: In this case, the rejection is extremely low and the solvent flow extremely high compared to the other membranes. Since lupanine is a base it may be further closing the polymer matrix having greater interaction with PBI.
3. Rejection: in respect of imprinted membranes, the amount of template is the same but, the value of rejection it's quite different. The rejection is greater on the imprinted membranes than on the non-imprinted membranes and lower when imprinted with the enantiomer L-(-)-Lupanine. Higher rejection values means that more Lupanine is retained. The high rejection value may mean the molecular recognition of the Lupanine molecule and when the membrane undergoes the x-link process, it causes the molecule to be further retained; for membrane imprinted with the enantiomer as a template, this rejection value may mean facilitated transport of the molecule. For membranes imprinted with the pure enantiomer, the enantiomeric excess of permeate and retentate was analyzed and both was found to be racemic mixture, i.e. there was no selectivity for only one enantiomer of lupanine as had been thought.

3.4- Resolution by formation of diastereomeric salts with or without PBI membranes

3.4.1- Optimization of diastereomeric resolution by recrystallization using as resolving agent TA and DTTA without PBI membranes

i. **Diastereomeric resolution by recrystallization with tartaric acid: screening of the best solvents:** Initially, three samples with different solvents: EtOH, MeOH and acetone were prepared. We started with 1g racemic lupanine and 1.1 mol equiv of L-tartaric acid.

Table 12- Sample of Lupanine with 1.1 mol equiv of L-tartaric acid

Sample	Concentration of lupanine (g/mL)	Solvent	Volume of solvent (mL)	Yield (%)	e.e (%)
A	0.334	Ethanol	7	9.47	20 % de D(+)
B	0.253	Methanol	6	21.47	Enantiomer D(+) pure
C	0.286	Acetone	6 (3+3)	Formation of a viscous solution	

As shows in table 4, methanol proved to be the best resolution solvent for the racemic lupanine with L-tartaric acid because it was obtained the D-(+)-Lupanine.

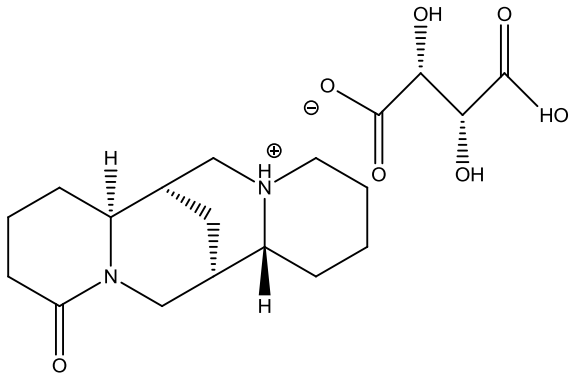

Fig. 38 - Formation of salt complex between Lupanine and L-tartaric acid

The figure 24 shows the interaction of the lupanine molecule with tartaric acid, where a salt complex is formed as lupaninium tartarate.

ii. **Diastereomeric resolution by recrystallization with Di-*p*-toluoyl-L-tartaric acid and Di-*p*-toluoyl-D-tartaric acid: screening of the best solvents:** Initially, four samples with different solvents: EtOH, MeOH, IPA and acetone were prepared. We started with 0.25g racemic lupanine and 1 mol equiv of L-DTTA or D-DTTA.

Table 13- Sample of Lupanine with D-DTTA and L-DTTA

Sample	Resolving agent	Solvent	Volume of solvent (mL)	e.e (%)
A1	D-DTTA	Methanol	2 (1+1)	No crystals
A2	D-DTTA	Acetone	2 (1+1)	89.6 of L-(-); White Crystals
	D-DTTA		2 (1+1)	57.6% of D-(+); Yellow Crystals
A3	D-DTTA	Isopropanol	5 (1+4)	No crystals
A4	D-DTTA	Ethanol	3 (1+2)	No crystals
A5	L-DTTA	Methanol	2 (1+1)	No crystals
A6	L-DTTA	Acetone	2 (1+1)	1.8 of L-(-)
A7	L-DTTA	Isopropanol	4 (1+3)	No crystals
A8	L-DTTA	Ethanol	3 (1+2)	No crystals

To improve the resolution process, recrystallization of racemic Lupanine with DTTA in different solvents such as EtOH, IPA, Methanol and Acetone was attempted. Both Lupanine and DTTA dissolved well in methanol but did not recrystallize. The same happened in the case of ethanol. In the experience with isopropanol, DTTA precipitated soon after we coupled DTTA with Lupanine. The only solvent which dissolved the two compounds well and recrystallized was acetone. With this, we have identified that acetone is the best solvent to be used in the recrystallization experiments of Lupanine with DTTA and therefore, all subsequent experiments were performed with this solvent.

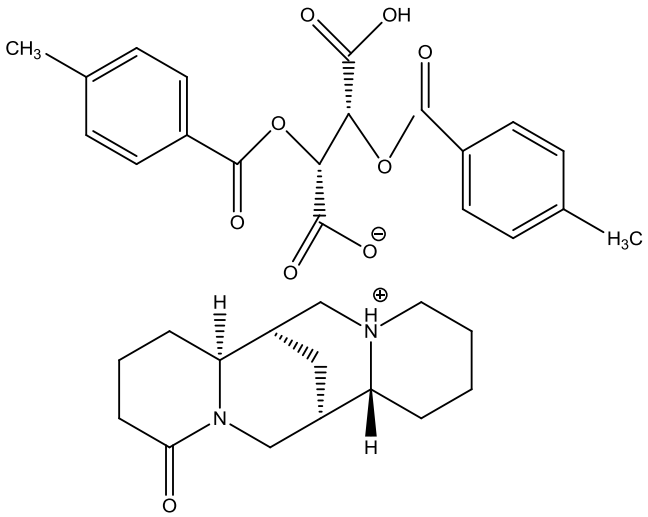

Fig. 39 - Formation of salt complex between Lupanine and L-DTTA

The figure above shows the interaction of the lupanine molecule with tartaric acid, where a salt complex is formed as lupaninium tartarate.

iii. **Diastereomeric resolution by recrystallization with Di-*p*-toluoyl-L-tartaric acid with the best solvent (acetone):** We started with 0.25g racemic lupanine and 1 mol equiv of L-DTTA in acetone.

Table 14- Samples of Lupanine with 1 mol equiv of L-DTTA in 2mL of acetone

Sample	Yield (%)	e.e (%)	[ ] Lupanine (g/mL)	[ ] DTTA (g/mL)	Days of Recrystallization
A	-	Racemic mixture	0.253	0.397	1
B	19.9	78.7 of L-Lupanine	0.253	0.397	2
C	15.7	79.5 of L-Lupanine	0.251	0.396	3
D	-	Racemic mixture	0.257	0.385	4
E	24.1	75.95 of L-Lupanine	0.193	0.077	2
F	18.3	83.16 of L-Lupanine	0.130	0.077	3

3.4.2- Resolution by formation of diastereomeric salts with PBI membranes

Membranes developed according to the procedure shown in Chapter 2.2.3 were used for this experiment, a NIM (non-imprinted), an MIM with racemic lupanine as a template and an MIM with D- (+) - Lupanine enantiomer as template, as well as without a membrane (blank).

We started with 1g racemic lupanine and 1.1 equiv L-(+)- tartaric acid. Lupanine was dissolved in 3mL of MeOH and tartaric acid in 4 mL IPA. The samples were recrystallized for 70 hours at room temperature.

Fig. 40- Illustration of recrystallization on membrane: membrane in contact with solution (left); formation of crystals (right)

Table 15- Samples of Lupanine with L-TA

Sample	Yield (%)	e.e (%)
A-MIM	58.57	Racemic mixture
B- MIM D- (+)-Lupanine	72.82	Racemic mixture
C- NIM	62.39	Racemic mixture
D- Glass support	30.27	Enantiomer D- (+) pure

The hypothesis of this experiment was whether the use of a membrane on assessing diastereomeric resolution could by its topology improve resolution. Crystal's formation was observed but as racemic mixture while the blank experiment, in glass support, gave pure enantiomer as expected.

Conclusion

We can conclude that the process of diastereomeric resolution by recrystallization of lupanine works better with tartaric acid than with DTTA. Indeed, the use of tartaric acid as resolving agent allows to obtain enantiomerically pure L-Lupanine. Still a low resolving yield was obtained. In the future, it should be try to optimize this process using mixtures of different solvents, both using tartaric acid and DTTA as resolving agents.

PBI beads were successfully used as a scavenger for lupanine. A initial attempt to recover lupanine from PBI beads using DCM as eluent was not efficient enough and further work requires to be done using different solvents, to improve lupanine recover and PBI regeneration.

The use of conditioned PBI proved to be extremely efficient in the removal of DMAP in DMAP / Meta solution, and it was later possible to recover most of the compounds through DCM and MeOH elution.PBI membranes were prepared and acidic or basic bath conditioned and assessed for DMAP removal as membrane adsorbers, and comparing with the conditioned beads. We can verify that the results are quite similar using the same amounts of PBI. However, the adsorption process with beads turns out to be a simpler process whereas the membranes have to be fabricated, being a process that takes at least 2 days. Another important aspect is the regeneration of PBI, in which we can reuse PBI. A factor to be explored in the future, both for beads and for membranes, that is, if we conserve to reuse and if the yield is the same.

Molecularly imprinted membranes for both racemic lupanine and template as for pure enantiomers exhibited low selectivity to lupanine, however, the use of these membranes for lupanine nanofiltration show very different rejections to lupanine implying that the introduction of this molecule in the dope solution when manufacturing these membranes affects greatly their permeation and selectivity properties.

The procedure of membrane recrystallization is still a recent concept. PBI membranes, as well as PBI membranes imprinting with pure or racemic lupanine. However, the results show, that in this case proved to be inefficient on increasing diastereomeric resolution efficiency, since crystals obtained were racemic.

References

[1] G. Székely, “Degenotoxification of pharmaceuticals by molecular imprinting and organic solvent nanofiltration,” 2012.

[2] R. Viveiros, M. Inês, W. Heggie, and T. Casimiro, “Green approach on the development of lock-and-key polymers for API purification,” *Chem. Eng. J.*, vol. 308, pp. 229–239, 2017.

[3] G. Szekely, M. C. A. De Sousa, M. Gil, F. C. Ferreira, and W. Heggie, “Genotoxic Impurities in Pharmaceutical Manufacturing : Sources , Regulations , and Mitigation,” *Chem. Rev.*, 2012.

[4] L. N. Nchari, “Molecular Mechanisms during Amplification of Chirality in Organometallic Systems : In Situ Studies by X-ray Absorption Spectroscopy,” 2010.

[5] L. A. Nguyen, H. He, and C. Pham-huy, “Chiral Drugs : An Overview,” *Int. J. Biomed. Sci. Chiral*, pp. 85–100, 2006.

[6] G. Gübitz and M. G. Schmid, *Chiral Separations Methods and Protocols*, vol. 243. 2004.

[7] L. Bingyun and D. T.Haynie, “Chiral Drug Separation,” in *Encyclopedia of Chemical Processing*, 2008, pp. 449–458.

[8] M. M. El-Shazly, “Improved Methodology for the Preparation of Chiral Amines,” 2009.

[9] O. Chuzel and O. Riant, “Sparteine as a Chiral Ligand for Asymmetric Catalysis,” in *Chiral Diazaligands for Asymmetric Synthesis*, M. Lemaire and P. Mangeney, Eds. Berlin, Heidelberg: Springer Berlin Heidelberg, 2005, pp. 59–92.

[10] N. J. Leonard, “Lupin Alkaloids,” in *The Alkaloids: Chemistry and Physiology*, pp. 119–199.

[11] A. N. Z. A. FOOD, “LUPIN ALKALOIDS IN FOOD A Toxicological Review and Risk Assessment,” 2001.

[12] C. Barbeitos, “Towards the development of a process for lupin beans detoxification wastewater with lupanine recovery,” 2016.

[13] A. K. Przyby and M. Kubicki, “Simple and highly ef fi cient preparation and characterization of (-) -lupanine and (+) -sparteine,” *Tetrahedron*, vol. 67, pp. 7787–7793, 2011.

[14] C. Afonso and N. Maulide, “Process for preparing enantiopure Lupanine and Sparteine.”

[15] M. D. de Pina, “Desenvolvimento de processos de adsorção molecular para remoção de impurezas genotóxicas de ingredientes farmacêuticos ativos,” *Master Thesis*, 2014.

[16] L. Müller, R. J. Mauthe, C. M. Riley, M. M. Andino, D. De Antonis, C. Beels, J. DeGeorge, A. G. M. De Knaep, D. Ellison, J. A. Fagerland, R. Frank, B. Fritschel, S. Galloway, E. Harpur, C. D. N. Humfrey, A. S. Jacks, N. Jagota, J. Mackinnon, G. Mohan, D. K. Ness, M. R. O’Donovan, M. D. Smith, G. Vudathala, and L. Yotti, “A rationale for determining, testing, and controlling specific impurities in pharmaceuticals that possess potential for genotoxicity,” *Regul. Toxicol. Pharmacol.*, vol. 44, no. 3, pp. 198–211, 2006.

[17] Vertellus, *DMAP Pharmaceuticals and Agrochemicals*. .

[18] E. Fritz, “MOLECULARLY IMPRINTED POLYMER BASED SCAVENGERS FOR PURIFYING SMALL AND LARGE ACTIVE PHARMACEUTICAL INGREDIENTS,” *PhD Thesis Fac. Chem. TU Dortmund*, 2014.

[19] G. Gu, “Chiral Separation by Chromatographic and Electromigration Techniques . A Review,” *Biopharm. Drug Dispos.*, vol. 336, no. May, pp. 291–336, 2001.

[20] “FDA Fundamentals.” [Online]. Available: http://www.fda.gov/AboutFDA/Transparency/Basics/ucm192695.htm.

[21] “PhRMA.” [Online]. Available: http://www.phrma.org/.

[22] “ICH.” [Online]. Available: http://www.ich.org/home.html.

[23] G. Q. Lin, J. G. Zhang, and J. F. Cheng, “Overview of Chirality and Chiral Drugs,” in *Chiral Drugs: Chemistry and Biological Action*, 2011, pp. 3–28.

[24] S. K. Branch, “13 International Regulation of Chiral Drugs 1,” *Chiral Sep. Tech. A Pract. Approach*, vol. 4, pp. 318–341, 2001.

[25] H. Caner, E. Groner, L. Levy, and I. Agranat, “Trends in the development of chiral drugs,” *Drug Discov. Today*, vol. 9, no. 3, pp. 105–110, 2004.

[26] R. L. Nation, “Chirality in New Drug Development Clinical Pharmacokinetic Considerations,” *Clin. Pharmacokinet.*, vol. 27, no. 4, pp. 249–255, 1994.

[27] T. Mcgovern and D. Jacobson-kram, “Regulation of genotoxic and carcinogenic impurities in drug substances and products,” *Trends Trends Anal. Chem.*, vol. 25, no. 8, pp. 790–795, 2006.

[28] D. Jacobson-Kram and A. Jacobs, “Use of genotoxicity data to support clinical trials or positive genetox findings on a candidate pharmaceutical or impurity .... now what?,” *Int. J. Toxicol.*, vol. 24, no. 3, pp. 129–34, 2005.

[29] D. Jacobson-Kram and T. McGovern, “Toxicological overview of impurities in pharmaceutical products,” *Adv. Drug Deliv. Rev.*, vol. 59, no. 1, pp. 38–42, 2007.

[30] A. Technologies, “Genotoxic impurities in pharmaceutical products.”

[31] B. S. Sekhon, “Exploiting the Power of Stereochemistry in Drugs : An Overview of Racemic and Enantiopure Drugs,” *J. Mod. Med. Chem.*, vol. 1, pp. 10–36, 2013.

[32] B. Gao, Y. Li, and K. Cui, “Molecularly imprinted membrane with innovative structure and high performance for chiral separation of amino acids,” *Int. J. Polym. Mater. Polym. Biomater.*, vol. 4037, no. July, pp. 0–48, 2017.

[33] B. Schuur and A. B. De Haan, *2.52 - Chiral Separations*, Second Edi., vol. 1. Elsevier B.V., 2011.

[34] L. M. Tam, “Designing crystallization based-enantiomeric separation for chiral compound-forming systems in consideration of polymorphism and solvate formation,” 2014.

[35] L. Chen and J. Li, “Recent advances in molecular imprinting technology : current status , challenges and highlighted applications,” *Chem Soc Rev*, vol. 40, pp. 2922–2942, 2011.

[36] G. Vasapollo, R. Del Sole, L. Mergola, M. R. Lazzoi, A. Scardino, S. Scorrano, and G. Mele, “Molecularly imprinted polymers: Present and future prospective,” *Int. J. Mol. Sci.*, vol. 12, no. 9, pp. 5908–5945, 2011.

[37] G. Wulff, “Molecular Imprinting in Cross-Linked Materials with the Aid of Molecular,” *Angew. Chemie Int. Ed. Engl.*, vol. 34, pp. 1812–1832, 1995.

[38] K. Mosbach, “Molecular imprinting,” *Trends Biochem. Sci.*, vol. 19, pp. 9–14, 1994.

[39] R. Xie, L.-Y. Chu, and J.-G. Deng, “Membranes and membrane processes for chiral resolution.,” *Chem. Soc. Rev.*, vol. 37, no. 6, pp. 1243–1263, 2008.

[40] C. Algieri, E. Drioli, L. Guzzo, and L. Donato, “Bio-mimetic sensors based on molecularly imprinted membranes,” *Sensors (Basel).*, vol. 14, no. 8, pp. 13863–13912, 2014.

[41] E. Chabanon and D. Mangin, “MEMBRANES & CRYSTALLIZATION PROCESSES : STATE OF THE ART & PROSPECTS,” *J. Memb. Sci.*, 2016.

[42] C. Charcosset, R. Kieffer, D. Mangin, and F. Puel, “Coupling between membrane processes and crystallization operations,” *Ind. Eng. Chem. Res.*, vol. 49, pp. 5489–5495, 2010.

[43] G. Di Profio, E. Curcio, and E. Drioli, “Membrane Crystallization Technology,” *Compr. Membr. Sci. Eng.*, vol. 3, pp. 21–46, 2010.

[44] M. Gil, W. Heggie, and F. C. Ferreira, “Environmental and economic analysis for selection and engineering sustainable API degenotoxification processes,” *Green Chem.*, vol. 15, pp. 210–225, 2013.

[45] C. Lee, R. Helmy, C. Strulson, J. Plewa, E. Kolodziej, V. Antonucci, B. Mao, C. J. Welch, Z. Ge, and M. A. Al-sayah, “Removal of Electrophilic Potential Genotoxic Impurities Using Nucleophilic Reactive Resins Abstract :,” no. December 2008, pp. 1021–1026, 2010.

[46] R. Kecili, J. Billing, D. Nivhede, B. Sellergren, A. Rees, and E. Yilmaz, “Fast identification of selective resins for removal of genotoxic aminopyridine impurities via screening of molecularly imprinted polymer libraries,” *J. Chromatogr. A*, vol. 1339, pp. 65–72, 2014.

[47] T. Esteves, R. Viveiros, J. Bandarra, W. Heggie, T. Casimiro, and F. Castelo, “Molecularly imprinted polymer strategies for removal of a genotoxic impurity , 4-dimethylaminopyridine , from an active pharmaceutical ingredient post-reaction stream,” *Sep. Purif. Technol.*, vol. 163, pp. 206–214, 2016.

[48] G. Szekely, M. F. Jimenez-Solomon, P. Marchetti, J. F. Kim, and A. G. Livingston, “Sustainability assessment of organic solvent nanofiltration: from fabrication to application,” *Green Chem.*, vol. 16, no. 10, pp. 4440–4473, 2014.

[49] N. H. H. Hairom, A. W. Mohammad, and A. A. H. Kadhum, “Nanofiltration of hazardous Congo red dye: Performance and flux decline analysis,” *J. Water Process Eng.*, vol. 4, no. C, pp. 99–106, 2014.

[50] L. Peeva, S. Burgal, I. Valtcheva, and A. G. Livingston, “Continuous purification of active pharmaceutical ingredients using multistage organic solvent nano fi ltration membrane cascade,” *Chem. Eng. Sci.*, vol. 116, pp. 183–194, 2014.

[51] “EQUILÍBRIO DE ADSORÇÃO E DE PERMUTA DE IÕES.” [Online]. Available: http://labvirtual.eq.uc.pt/siteJoomla/index.php?Itemid=450&id=188&option=com_content&task=view.

[52] J. P. Simonin, “On the comparison of pseudo-first order and pseudo-second order rate

laws in the modeling of adsorption kinetics," *Chem. Eng. J.*, vol. 300, pp. 254–263, 2016.

[53] N. F. Cardoso, "Remoção do Corante Azul de Metileno de Efluentes Aquosos Utilizando Casca de Pinhão in Natura e Carbonizada como Adsorvente," 2010.

[54] A. Sannigrahi, D. Arunbabu, R. Murali Sankar, and T. Jana, "Aggregation behavior of polybenzimidazole in aprotic polar," *Macromolecules*, vol. 40, no. 8, pp. 2844–2851, 2007.

[55] P. Taylor, "A Critical Review of Polybenzimidazoles : Historical Development and Future R & D," vol. 1797, no. 779749116, 1997.

[56] I. B. Valtcheva, S. C. Kumbharkar, J. F. Kim, Y. Bhole, and A. G. Livingston, "Beyond polyimide: Crosslinked polybenzimidazole membranes for organic solvent nanofiltration (OSN) in harsh environments," *J. Memb. Sci.*, vol. 457, pp. 62–72, 2014.

[57] F. C. Ferreira, T. Esteves, A. . Vicente, and C. A. . Afonso, "Polímero de polibenzimidazolo com cadeia espaçadora e seu método de obtenção para remoção de impurezas genotóxicas," 2016.

Annex

Annex 1- Calibrations curves

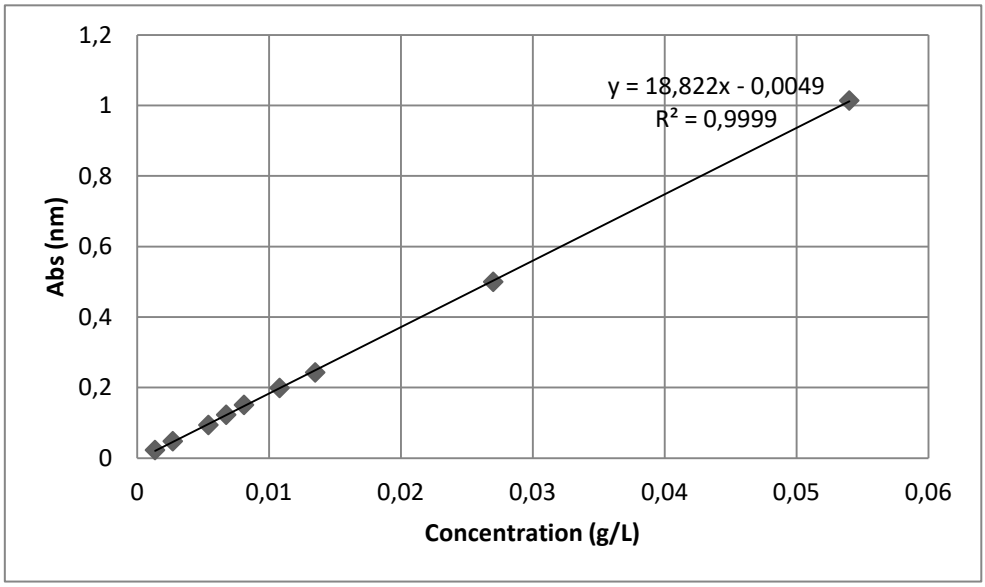

Fig. 41 - Calibration curve of Brilliant Blue in MeCN

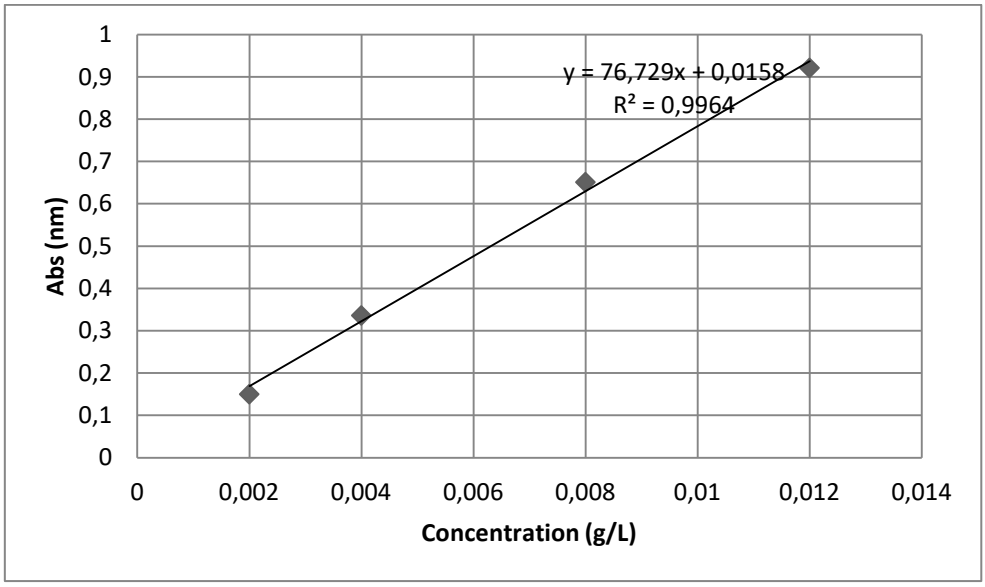

Fig. 42 - Calibration curve of Polystyrene 580 in MeCN

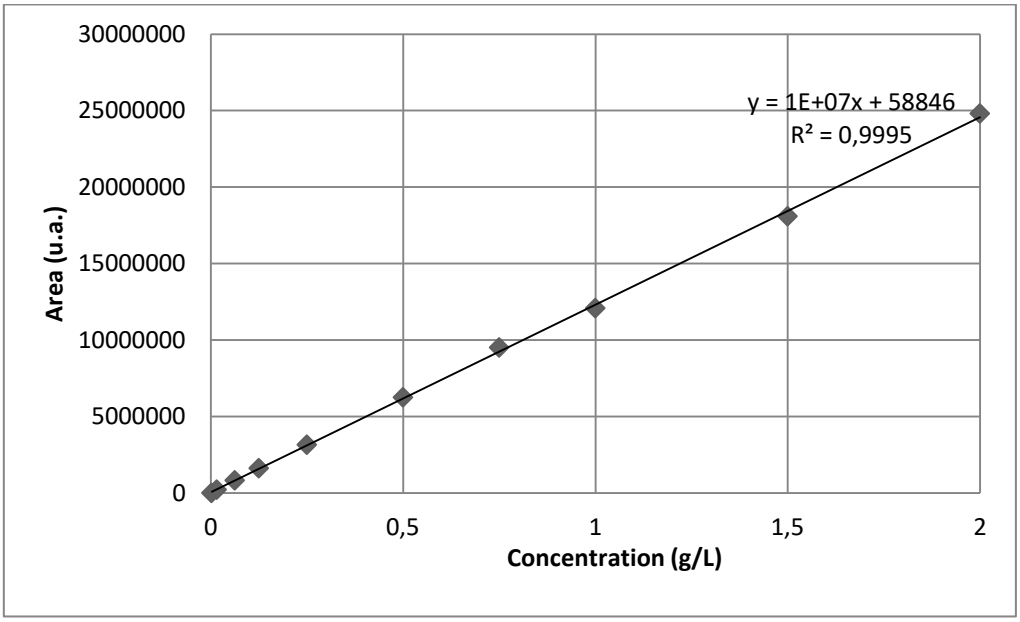

Fig. 43 - Calibration curve of Lupanine in H_2O for lower integrations of 24809353 u.a.

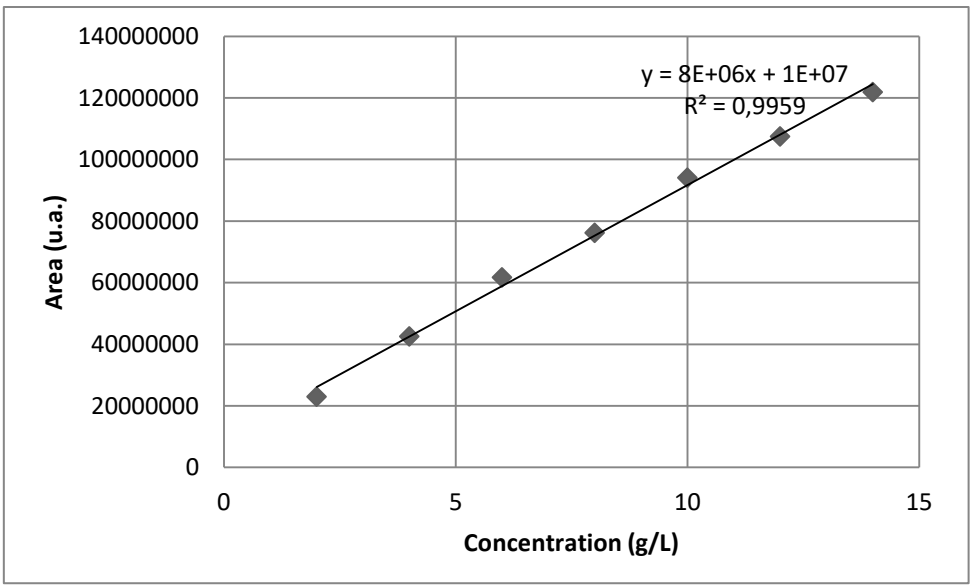

Fig. 44 - Calibration curve of Lupanine in H_20 for higher integrations of 24809353 u.a.

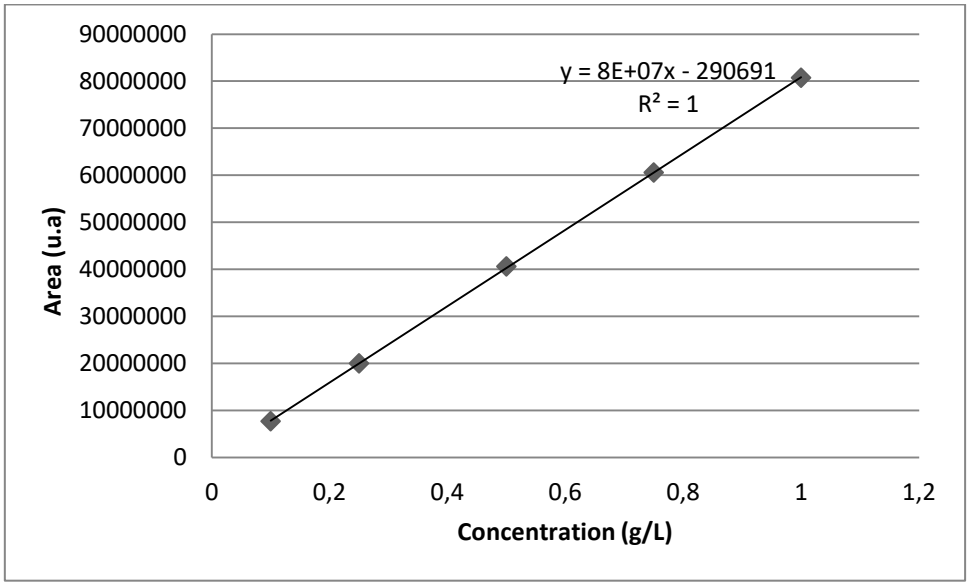

Fig. 45 - Calibration curve of DTTA

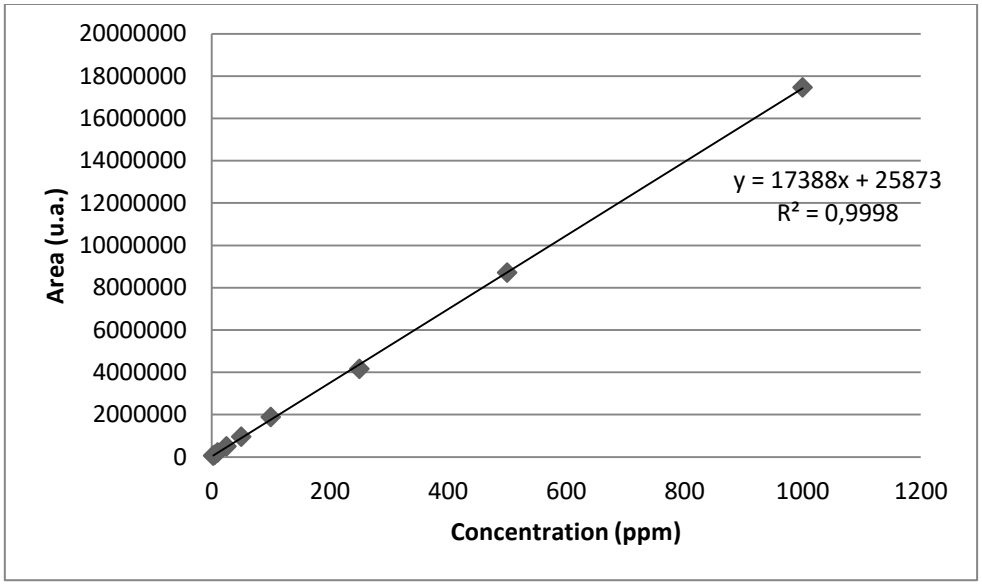

Fig. 46 - Calibration curve of Meta in DCM (concentration between 2.5 to 1000 ppm)

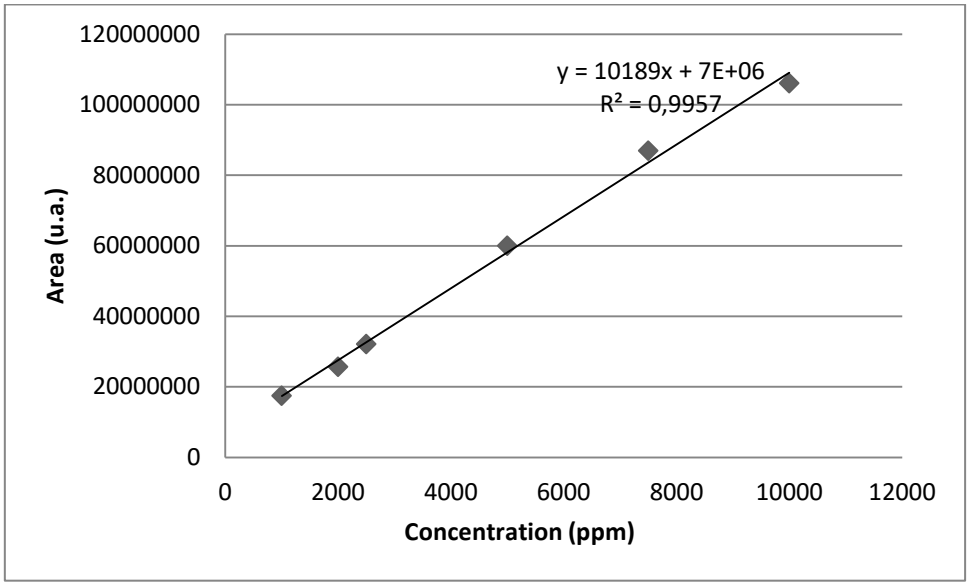

Fig. 47- Calibration curve of Meta in DCM (concentration between 1000 to 10000 ppm)

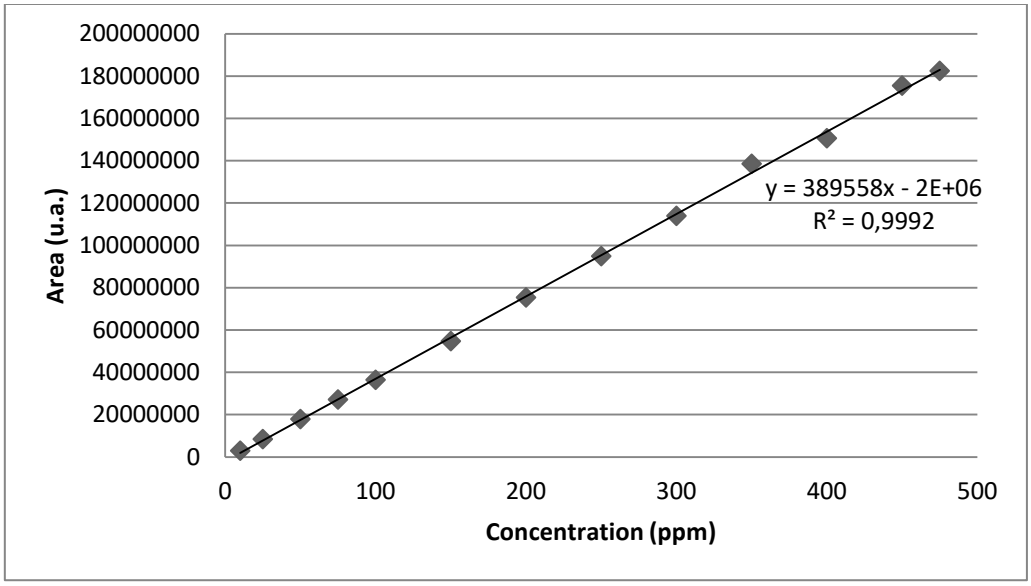

Fig. 48 - Calibration curve of DMAP in DCM (concentrations between 10 and 475 ppm)

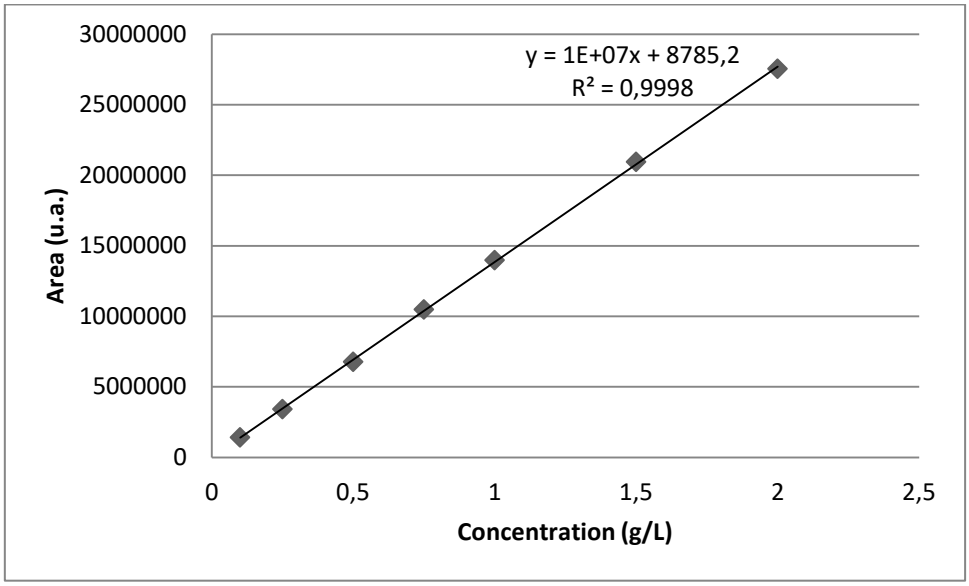

Fig. 49- Calibration curve of L-tartaric acid in water

Annex 2- Adsorption isotherms and kinetics

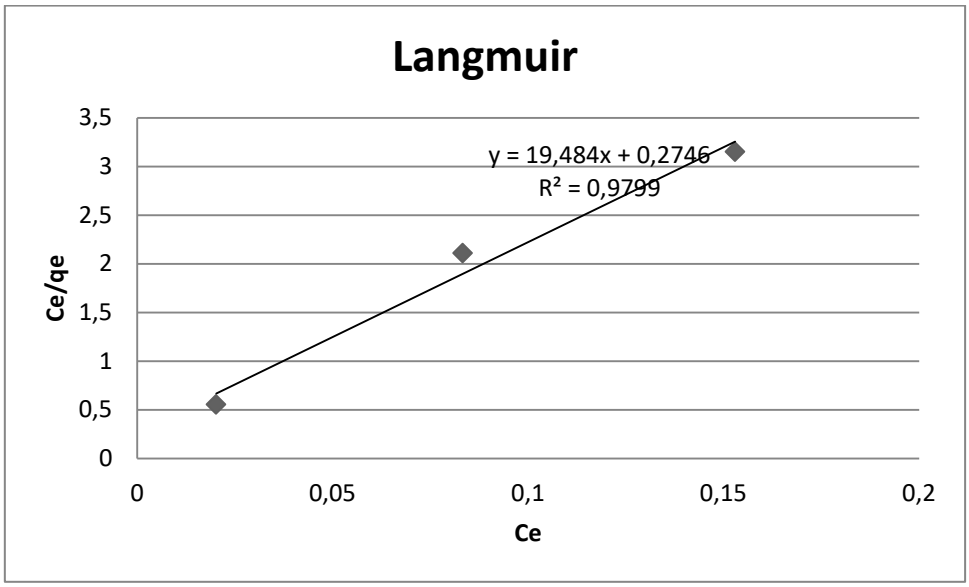

Fig. 50- Langmuir isotherm for binding of PBI-COOH with Lupanine in water

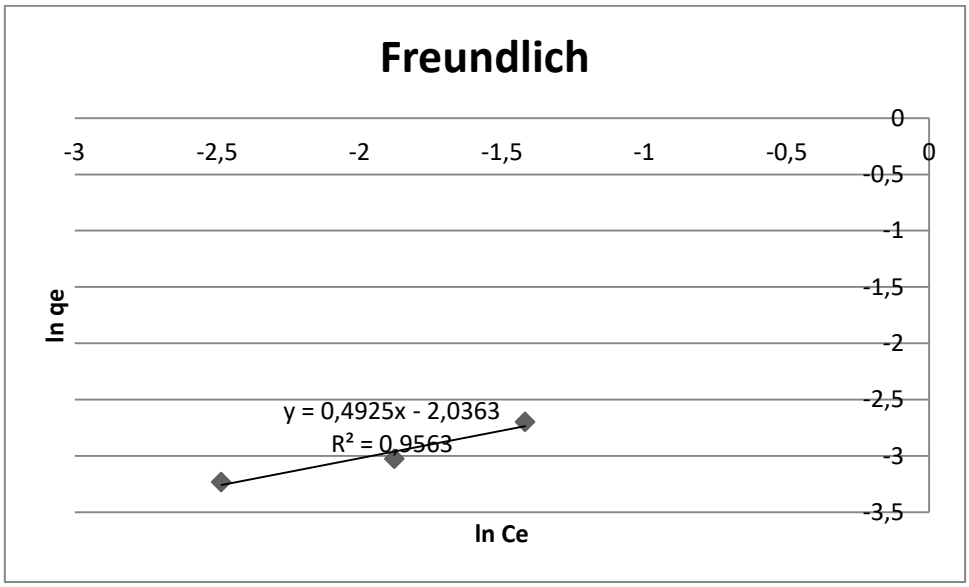

Fig. 51- Freundlich isotherm for binding of PBI-COOH with Lupanine in water

Table 16- Parameters of the theoretical adsorption models obtained for a Lupanine solution in water with PBI-COOH

Langmuir			Freundlich		
q_{max} (g/g)	K_L (g/L)	R^2	K_F (g/L)	1/n	R^2
0.051	70.95	0.979	0.141	0.546	0.956

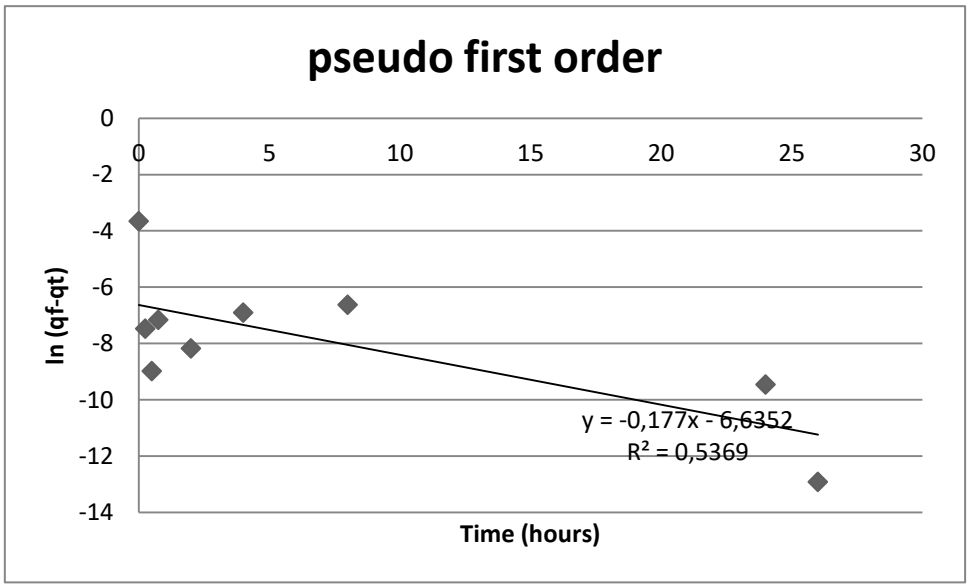

Fig. 52 - Pseudo first order kinetic for binding of PBI-COOH with Lupanine in water

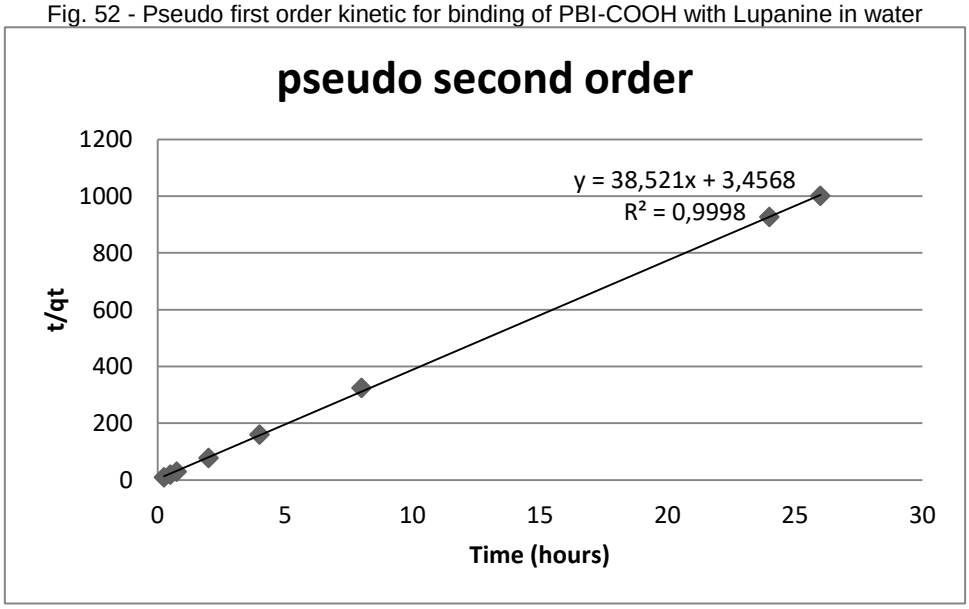

Fig. 53- Pseudo second order kinetic for binding of PBI-COOH with Lupanine in water

Table 17- Parameters of the theoretical kinetics models obtained for a Lupanine solution in water with PBI-COOH

Pseudo first order			**Pseudo second order**		
K_1 (h^{-1})	**qf (g/g)**	**R^2**	**K_2 ($mg^{-1}.h^{-1}$)**	**qf (g/g)**	**R^2**
0.177	0.0013	0.537	0.000195	0.0263	0.999

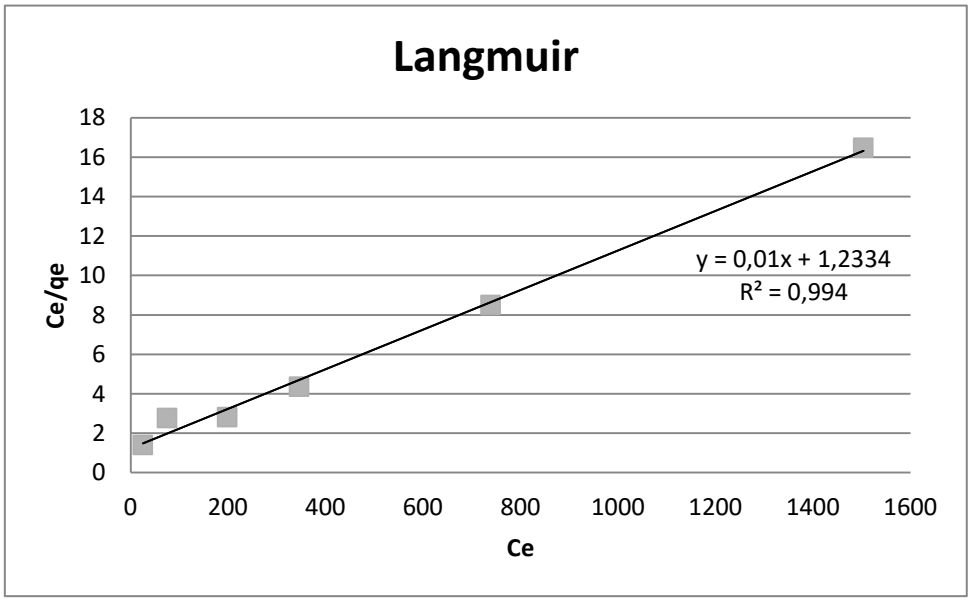

Fig. 54- Langmuir isotherm for binding of PBI-TA with DMAP in DCM

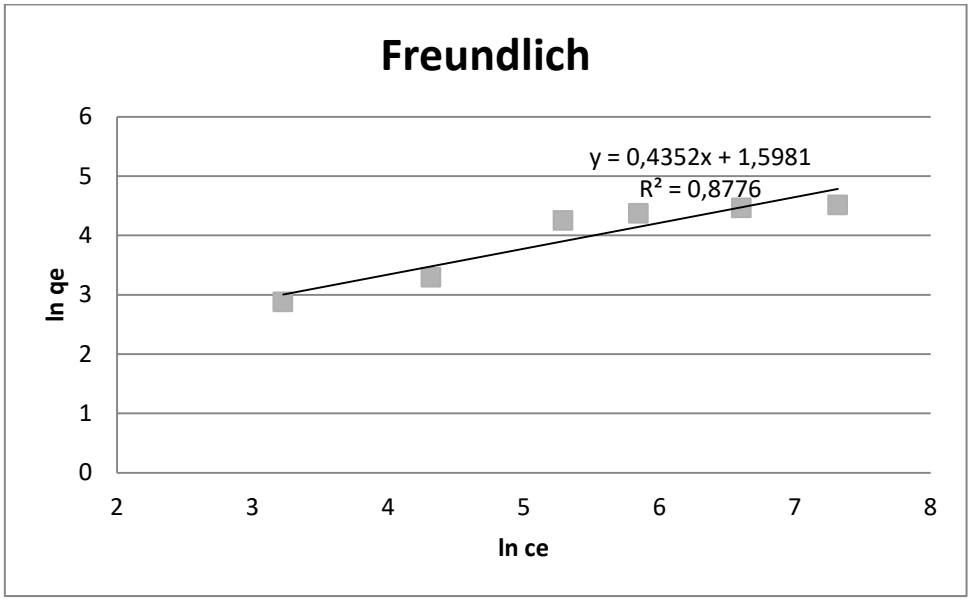

Fig. 55- Freundlich isotherm for binding of PBI-TA with DMAP in DCM

Table 18- Parameters of the theoretical isothermic models obtained for DMAP in DCM with PBI-TA

Langmuir			**Freundlich**		
q_{max} (g/g)	**K_L (g/L)**	**R^2**	**K_F (g/L)**	**1/n**	**R^2**
100.000	0.008	0.994	4.944	0.435	0.877

Table 19- Parameters of the theoretical kinetics models obtained for DMAP in DCM with PBI-TA

Pseudo first order			Pseudo second order		
K_1 (h^{-1})	qf (g/g)	R^2	K_2 ($mg^{-1}.h^{-1}$)	qf (g/g)	R^2
0.066	0.0066	0.1350	551.517	0.1672	1.000

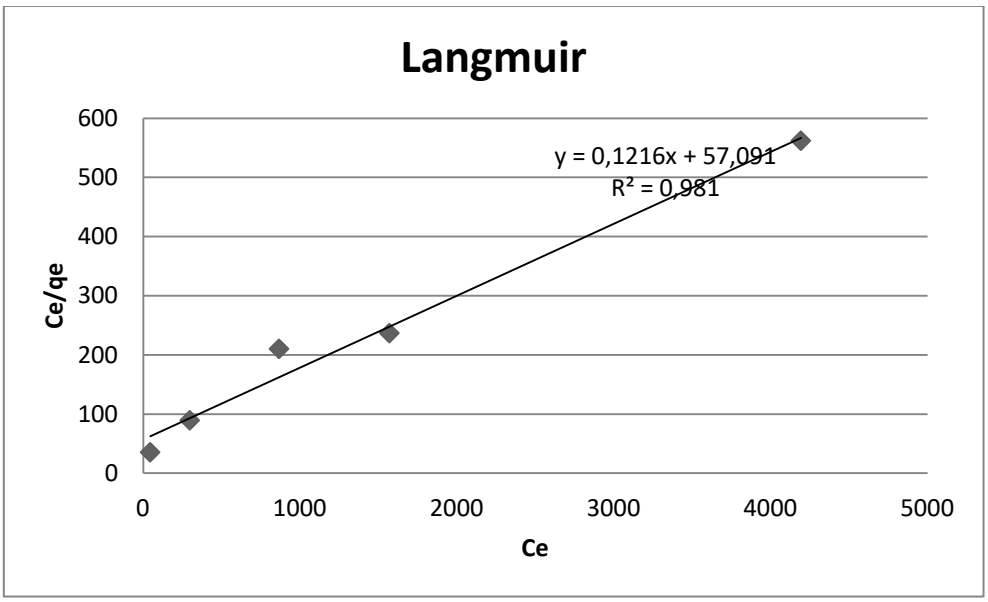

Fig. 56- Langmuir isotherm for binding of PBI-TA with Meta in DCM

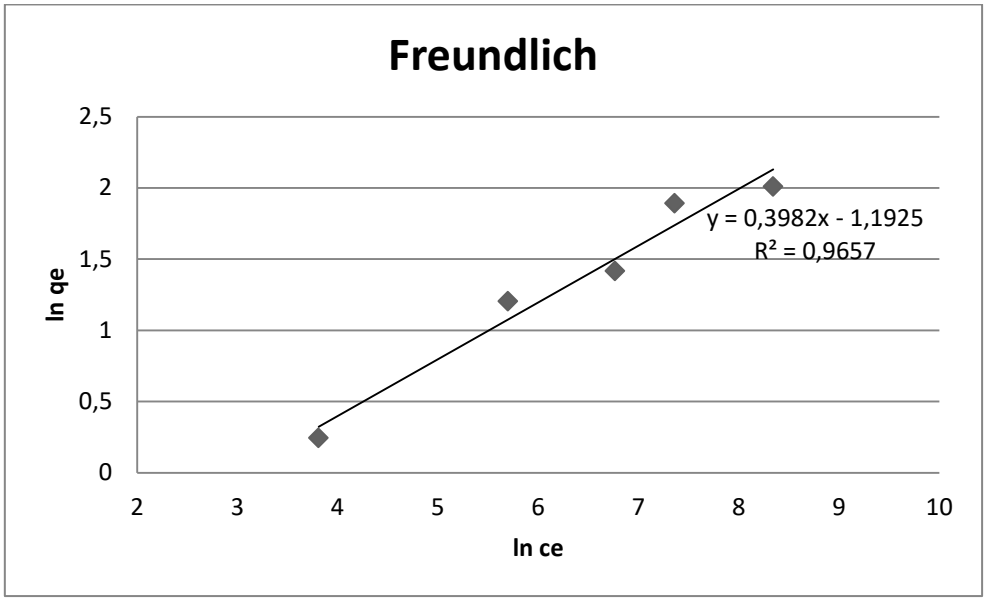

Fig. 57- Freundlich isotherm for binding of PBI-TA with Meta in DCM

Table 20- Parameters of the theoretical isothermic models obtained for Meta in DCM with PBI-TA

Langmuir			**Freundlich**		
q_{max} (g/g)	**K_L (g/L)**	**R^2**	**K_F (g/L)**	**1/n**	**R^2**
8.224	0.002	0.981	0.303	0.389	0.966

Annex 3- PBI modifications and possible chemical interactions with other molecules

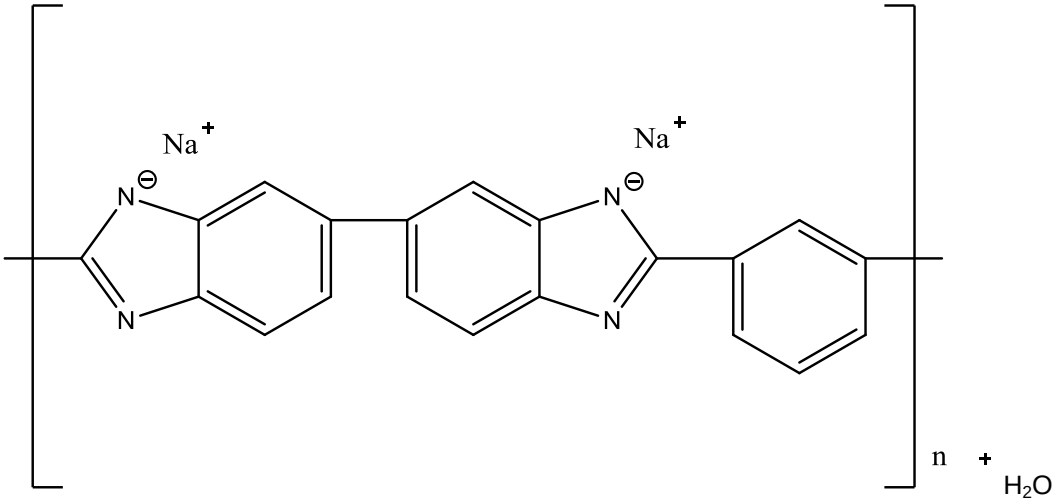

Fig. 58- PBI-TB

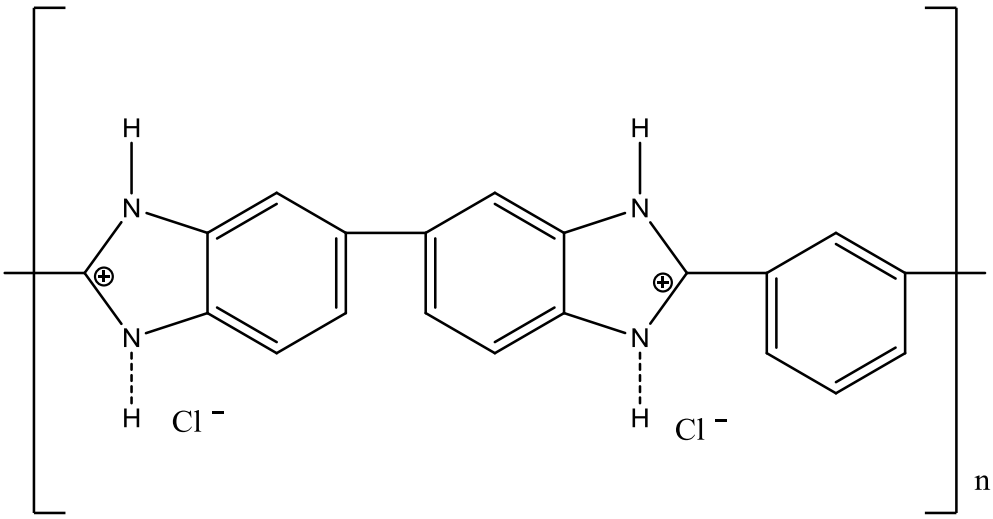

Fig. 59- PBI-TA

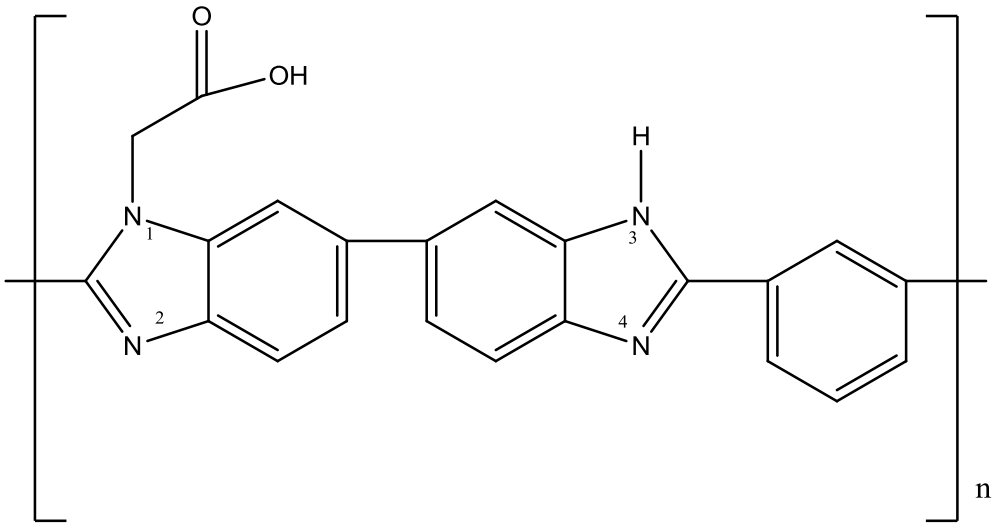

Fig. 60- PBI-COOH

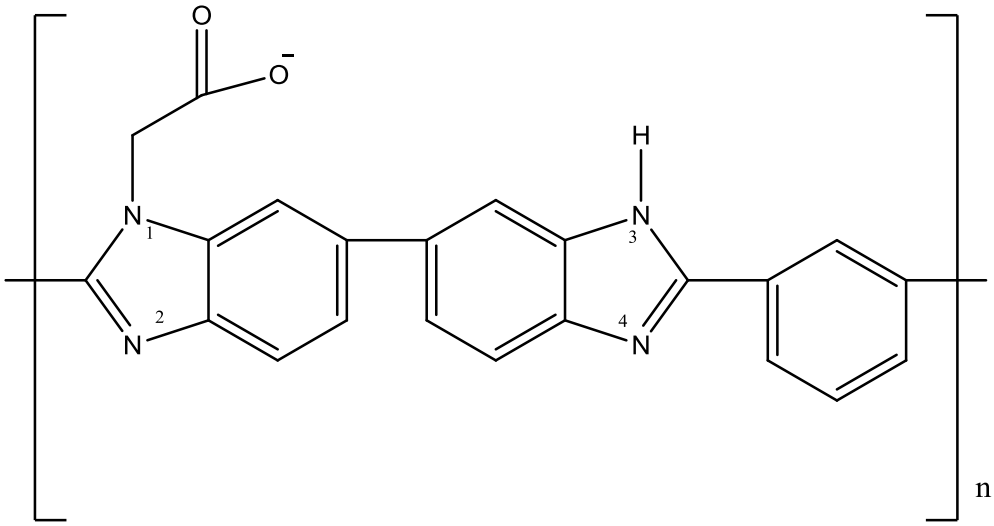

Fig. 61- PBI-COOH deprotonated

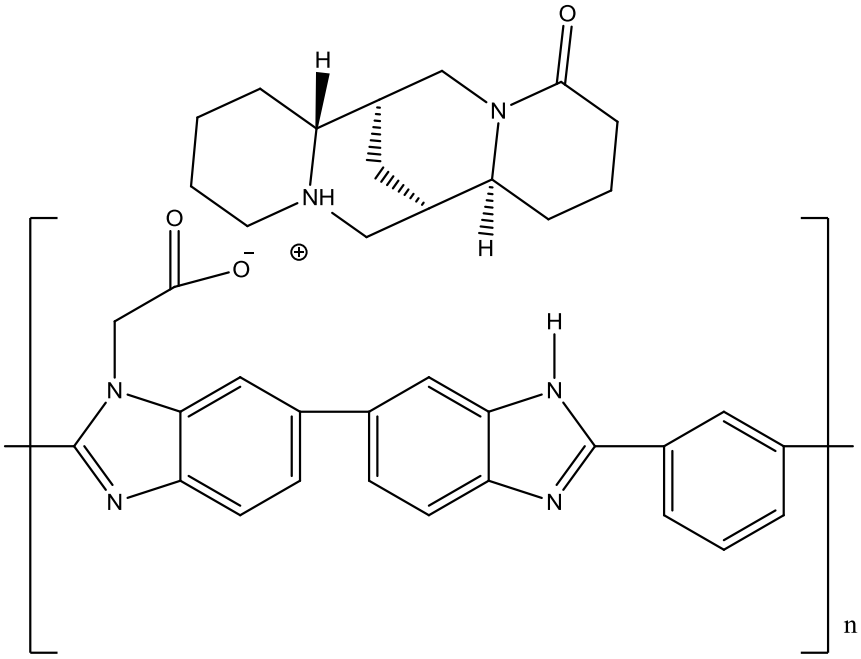

Fig. 62- PBI-COOH deprotonated with protonated Lupanine

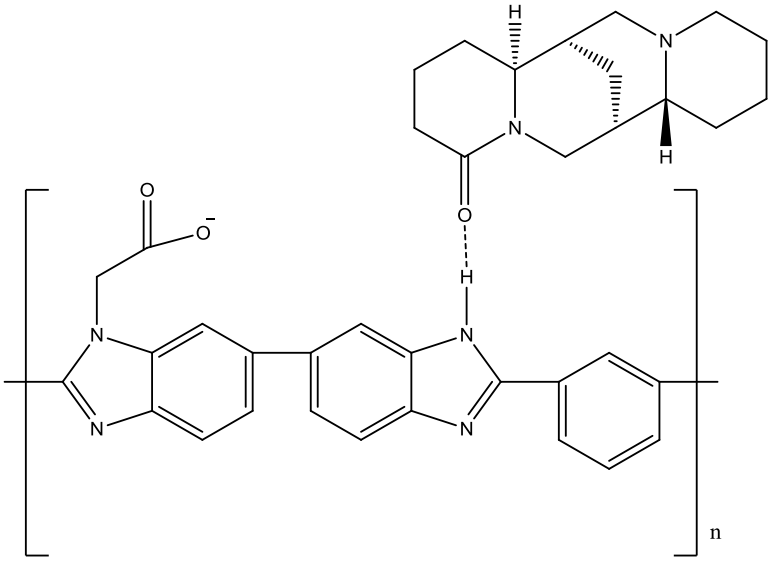

Fig. 63- PBI-COOH deprotonated with Lupanine

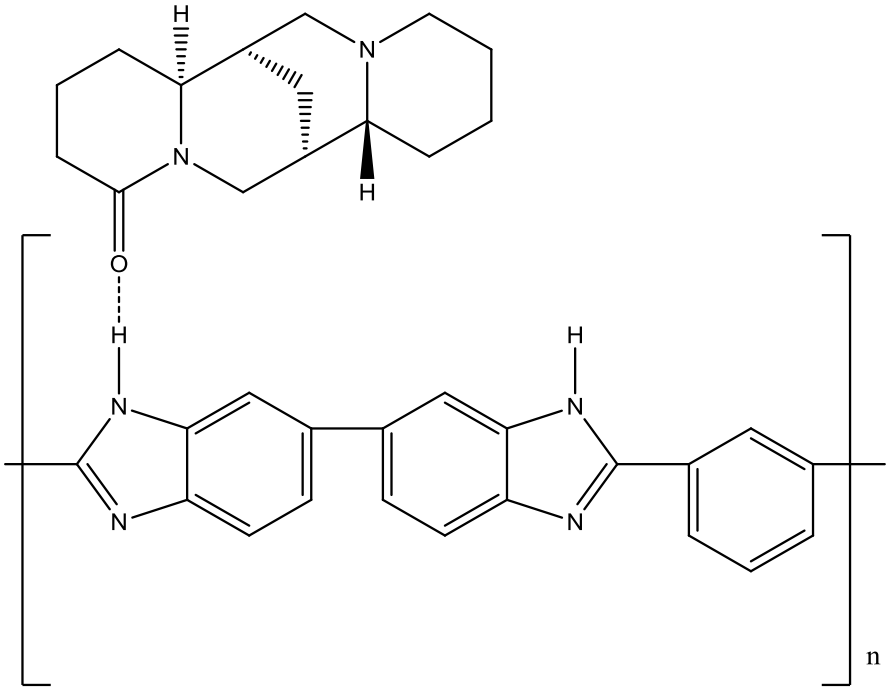

Fig. 64- PBI-T with Lupanine

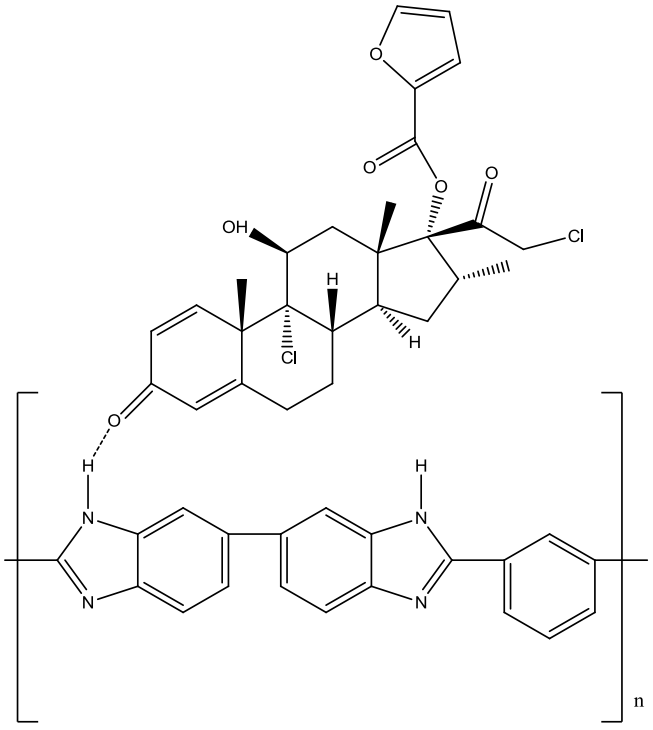

Fig. 65- PBI-T with Meta

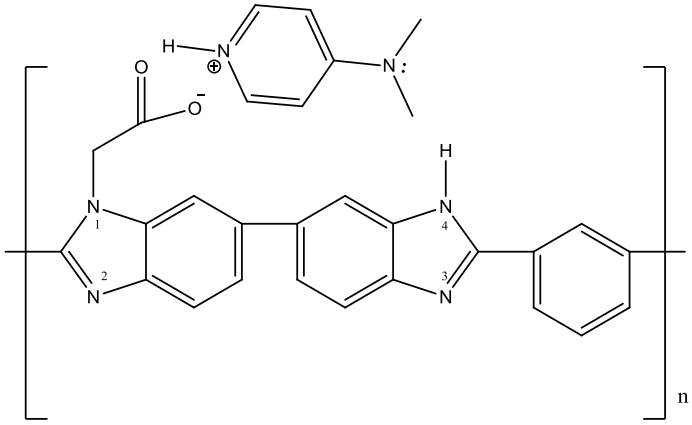

Fig. 66- PBI-COOH deprotonated with DMAP protonated

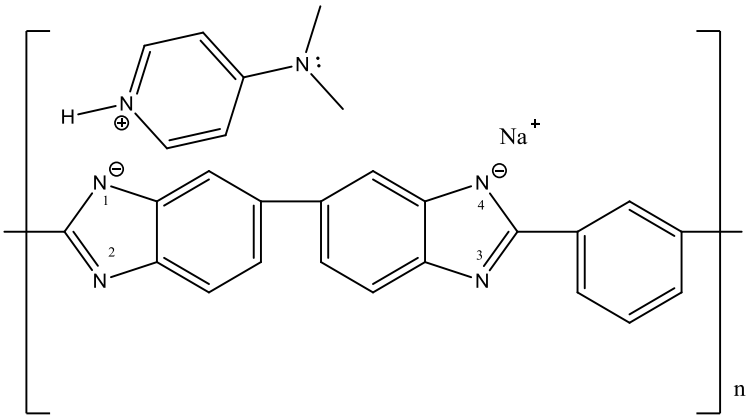

Fig. 67- PBI-TB with DMAP protonated

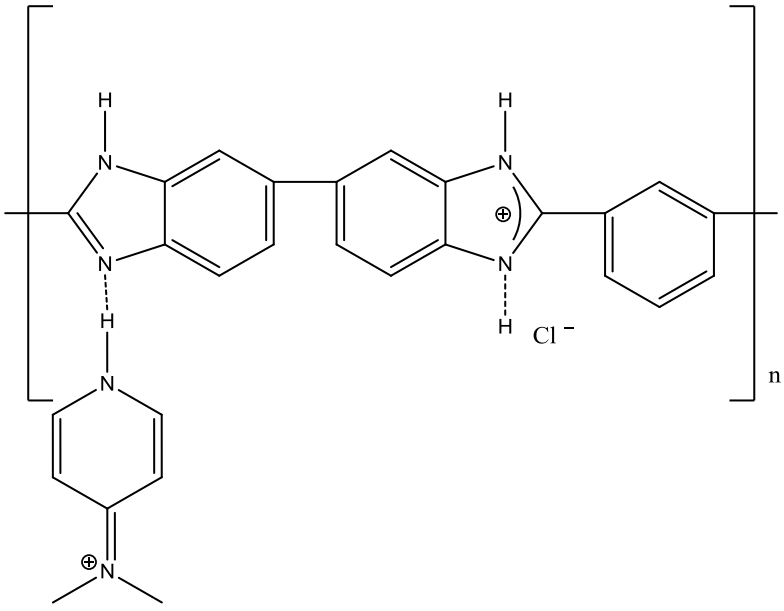

Fig. 68- PBI-TA with DMAP